ELSEVIER

Computers and Chemical Engineering 24 (2000) 2633–2654

Computers & Chemical Engineering

www.elsevier.com/locate/compchemeng

Comparison of finite difference and control volume methods for solving differential equations

Gerardine G. Botte, James A. Ritter, Ralph E. White *

Department of Chemical Engineering, Center for Electrochemical Engineering, University of South Carolina, Columbia, SC 29208, USA

Received 5 May 1998; received in revised form 10 August 2000; accepted 11 August 2000

Abstract

Comparisons are made between the finite difference method (FDM) and the control volume formulation (CVF). An analysis of truncation errors for the two methods is presented. Some rules-of-thumb related to the accuracy of the methods are included. It is shown that the truncation error is the same for both methods when the boundary conditions are of the Dirichlet type, the system equations are linear and represented in Cartesian coordinates. A technique to analyze the accuracy of the methods is presented. Two examples representing different physical situations are solved using the methods. The FDM failed to conserve mass for a small number of nodes when both boundary conditions include a derivative term (i.e. either a Robin or Neumann type boundary condition) whereas the CVF method did conserve mass for these cases. The FDM is more accurate than the CVF for problems with interfaces between adjacent regions. The CVF is (ΔX) order of accuracy for a Neumann type boundary condition whereas the FDM is $(\Delta X)^2$ order.

Keywords: Finite difference method; Control volume formulation; Truncation errors; Stepwise profile; Piecewise-linear profile; Taylor's series

1. Introduction

The finite difference method (FDM) is a popular numerical technique for solving systems of differential equations that describe mass, momentum, and energy balances. Its development began at the end of the 1940s (Ciarlet & Lions, 1990), and is very well established by now. In the FDM, the differential equation is approximated by a set of algebraic equations using a Taylor-Series expansion where the accuracy is improved with the use of more terms in the series and with the use of small grid spacing sizes (i.e. a large number of nodes). The simplicity of this method has made it a very useful technique in many different fields. However, it has been pointed out (Patankar, 1980; West & Fuller, 1996; West, Yang & Debecker, 1995) that the FDM sometimes yields unrealistic behavior and that mass is only rigorously conserved in the limit when the grid spacing goes to zero (Patankar, 1980; West & Fuller, 1996). To circumvent these situations, some investigators have used the control volume formulation (CVF, Patankar, 1980; West & Fuller, 1996; West et al., 1995). The origin of the CVF, or finite volume method (FVM) as it is also known, can be traced to Varga (1965) who refers to the CVF method as the Integration Method. Varga states that the Integration Method seems to have arisen as a result of numerical investigations of heterogeneous reactor problems (Stark, 1956; Tikhonov & Samarskii, 1956; Varga, 1957; Marchuk, 1959; Wachspress, 1960). Davis (1984) recommends the use of the Integration Method, for interfaces between adjacent regions. Most of the recent applications of the CVF are in computational fluid dynamics (Vijayan & Kallinderis, 1994; Versteeg & Malalasekera, 1995; Moder, Chai, Parthasarathy, Lee & Patankar, 1996; Cordero, De Biase & Pennati, 1997; Baek, Kim & Kim, 1998; Noh & Song, 1998; Shahcheragui & Dwyer, 1998; Thynell, 1998; Chan & Anastasiou, 1999; Munz, Schneider, Sonnendrucker, Stein, Voss & Westermann, 1999; Sohankar, Norberg & Davison, 1999; Su, Tang & Fu, 1999).

In the CVF method, the differential equation is integrated over a control volume and the resultant equation is discretised using some special approximations, which

* Corresponding author. Tel.: +1-803-7773270; fax: +1-803-7778265.

E-mail address: rew@sc.edu (R.E. White).

0098-1354/00/$ - see front matter
PII: S0098-1354(00)00619-0

are discussed further below (see also Patankar, 1980). Since the CVF utilizes integration over small control volumes and since the flux of material at the common face between two adjacent control volumes is represented by the same expression, material is rigorously conserved (West & Fuller, 1996).

The objective of this paper is to compare the FDM to the CVF in terms of their accuracy, conservation of mass, and execution time. A general analysis of errors is used to study the accuracy of the methods. It is shown that the truncation errors are the same for the approximations of the second and first derivatives for both methods in the central nodes (FDM) or internal control volumes (CVF). It was reported incorrectly before by others (Leonard, 1994, 1995; Leonard & Mokhtari, 1990) that the truncation errors for the first and second derivatives obtained for the CVF method are smaller than that for the FDM. The effect of the boundary conditions on the accuracy of the solution is also shown in the analysis of errors. Two examples representing different physical situations are treated using the two methods.

2. Description of the methods

2.1. FDM

The FDM method consists of replacement of continuous variables by discrete variables; that is, instead of obtaining a solution, which is continuous over the whole domain of interest, the FDM yields values at discrete points. In the FDM a differential equation is approximated by a set of linear algebraic equations using a Taylor Series expansion. For nonlinear systems, after discretisation of the equations, a set of nonlinear algebraic equations is obtained, which can be solved using Newton's method (Davis, 1984; White, 1987).

Once the equations have been discretised, the resulting set of algebraic equations are solved simultaneously by using different packages such as Maple, Math-Cad, etc. (Abell & Braselton, 1994; Mathcad7, 1997). For this paper, we used the subroutine BAND (J) (Newman, 1967, 1968, 1973a,b) and Maple (Abell & Braselton, 1994) to solve the algebraic equations.

The accuracy of the FDM depends on the fixed grid spacing (the smaller the grid spacing the better the accuracy), and the number of the terms used in the Taylor series (the more terms the better the accuracy). Different discretisations can be used depending on the situation and the accuracy required by the process, i.e. high order discretisations have been used successfully in electrochemical systems (Van Zee, Kleine & White, 1984; Fan & White, 1991). As shown in Fig. 1a, we use the three-point forward, three-point backward and three-point central difference approximations for the derivatives (these approximations yield an accuracy of order $(\Delta X)^2$). More details are readily available about the FDM (Ciarlet & Lions, 1990; Pozrikidis, 1997, 1998). The discretised equations for the approximations using FDM are given in Table 1.

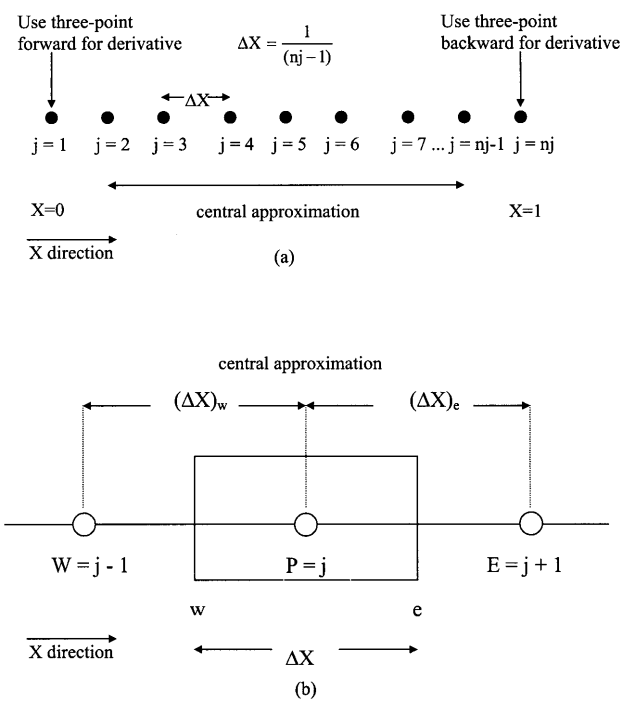

Fig. 1. Comparison of the FDM and CVF discretisation methods (a) typical discretisation with FDM, (b) typical one-dimensional control volume with CVF.

2.2. CVF

In the CVF the differential equation is integrated over a control volume, and the resultant equation is discretised using assumed approximations or profiles (Patankar, 1980; Versteeg & Malalasekera, 1995). Fig. 1b shows a typical one dimensional control volume for the CVF. Integration of the first and second order derivatives using the control volume shown in Fig. 1b yields:

$$\int_w^e \frac{d\phi}{dX}\,dX = \phi_e - \phi_w \tag{1}$$

$$\int_w^e \frac{d^2\phi}{dX^2}\,dX = \frac{d\phi}{dX}\Big|_e - \frac{d\phi}{dX}\Big|_w \tag{2}$$

The CVF method also yields values at node points. In this case the node points are labeled W, P, and E (see Fig. 1b). Values for ϕ at these node points can be obtained by assuming a profile for ϕ between the node

Table 1
Discretised equation of the different models for the derivatives and/or variable using FDM and CVF

Model of	Method	Approximation	Equations
$\frac{d\phi}{dX}$ (Left boundary)	FDM	$\frac{-3\phi_1+4\phi_2-\phi_3}{2\Delta X}$	T1.1
$\frac{d\phi}{dX}$ (Right boundary)	FDM	$\frac{3\phi_{nj}-4\phi_{nj-1}+\phi_{nj-2}}{2\Delta X}$	T1.2
$\frac{d\phi}{dX}$ (Governing equation)	FDM	$\frac{\phi_{j+1}-\phi_{j-1}}{2\Delta X}$	T1.3
$\frac{d^2\phi}{dX^2}$ (Governing equation)	FDM	$\frac{\phi_{j+1}-2\phi_j+\phi_{j-1}}{\Delta X^2}$	T1.4
$\frac{1}{\Delta X}\frac{d\phi}{dX}\Big\|_e$	CVF-PLP	$\frac{\phi_{j+1}-\phi_j}{\Delta X^2}$	T1.5
$\frac{1}{\Delta X}\frac{d\phi}{dX}\Big\|_w$	CVF-PLP	$\frac{\phi_j-\phi_{j-1}}{\Delta X^2}$	T1.6
$\frac{1}{\Delta X}\frac{d\phi}{dX}\Big\|_e-\frac{1}{\Delta X}\frac{d\phi}{dX}\Big\|_w$	CVF-PLP	$\frac{\phi_{j+1}-2\phi_j+\phi_{j-1}}{\Delta X^2}$	T1.7
$\frac{\phi_e}{\Delta X}$	CVF-PLP	$\frac{\phi_{j+1}+\phi_j}{2\Delta X}$	T1.8
$\frac{\phi_w}{\Delta X}$	CVF-PLP	$\frac{\phi_{j-1}+\phi_j}{2\Delta X}$	T1.9
$\frac{\phi_e}{\Delta X}-\frac{\phi_w}{\Delta X}$	CVF-PLP	$\frac{\phi_{j+1}-\phi_{j-1}}{2\Delta X}$	T1.10
$\frac{\phi_e}{\Delta X}$	CVF-SP	$\frac{\phi_j}{\Delta X}$	T1.11
$\frac{\phi_w}{\Delta X}$	CVF-SP	$\frac{\phi_{j-1}}{\Delta X}$	T1.12
$\frac{\phi_e}{\Delta X}-\frac{\phi_w}{\Delta X}$	CVF-SP	$\frac{\phi_j-\phi_{j-1}}{\Delta X}$	T1.13

points. Fig. 2a shows the results of assuming a stepwise profile (SP) and Fig. 2b shows the results for a piecewise linear profile (PLP). It is important to note that the assumed profile for ϕ_e and ϕ_w can be different from that assumed for $d\phi/dX|_e$ and $d\phi/dX|_w$. The SP (or upwind) profile is usually used to represent the variable, and the PLP is used to represent the derivative of the variable. More accurate, higher order discretisation schemes have been used successfully for the CVF method (Leonard, 1994, 1995; Leonard & Mokhtari, 1990; Johnson & Mackinnon, 1992; Castillo, Hyman, Shashkow & Steinberg, 1995).

In this study, the points 'W', 'P' and 'E' are considered equidistant and the points 'w' and 'e' are fixed half way between the points 'W–P' and 'P–E', respectively (see Fig. 2a); therefore, $(\Delta X)_e=(\Delta X)_w=\Delta X$. This assumption makes the equations of the CVF comparable with the discretisations used in the FDM presented above. The values used for ϕ_e and ϕ_w depend on the assumed profile.

$$\phi_e=\phi_p=\phi_j \quad \text{for SP} \tag{3}$$

$$\phi_w=\phi_W=\phi_{j-1} \quad \text{for SP} \tag{4}$$

$$\phi_e=\frac{\phi_P+\phi_E}{2}=\frac{\phi_j+\phi_{j+1}}{2} \quad \text{for PLP} \tag{5}$$

$$\phi_w=\frac{\phi_P+\phi_W}{2}=\frac{\phi_j+\phi_{j-1}}{2} \quad \text{for PLP} \tag{6}$$

The approximations for the derivatives are obtained from the assumed PLP.

$$\frac{d\phi}{dX}\Big|_e=\frac{\phi_E-\phi_P}{\Delta X}=\frac{\phi_{j+1}-\phi_j}{\Delta X} \quad \text{for PLP only} \tag{7}$$

$$\frac{d\phi}{dX}\Big|_w=\frac{\phi_P-\phi_W}{\Delta X}=\frac{\phi_j-\phi_{j-1}}{\Delta X} \quad \text{for PLP only} \tag{8}$$

The discretised equations for the CVF approximations are summarized in Table 1.

When the equation of interest involves time dependence (unsteady state), the implicit stepping method satisfies the physical behavior of the function, and the resulting equations are very simple (Patankar, 1980).

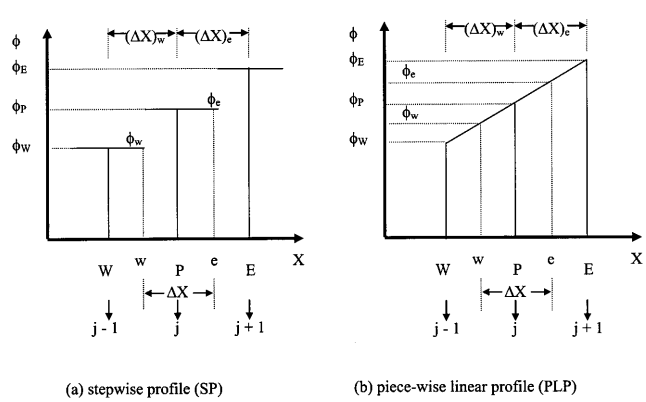

Fig. 2. Typical profiles use in the control volume formulation.

The implicit stepping scheme is thus used here and is given by

$$\int_t^{t+\Delta t} \phi \, dt = \phi|_{t+\Delta t} - \phi|_t \tag{9}$$

More details about the CVF are available elsewhere (Patankar, 1980; Versteeg & Malalasekera, 1995).

3. Results and discussion

We have divided the results in two sections (1) Truncation errors, and (2) examples. In the first section a general analysis of the truncation error of the approximations is made in order to analyze the accuracy of the techniques, and in the second section two examples representing different physical situations are presented to compare the FDM and CVF. The examples include an unsteady-state convective diffusion equation (example 1), and a steady-state heat conduction with a forcing function (example 2). Example 1 is used to verify the mass conservativeness of the methods, and example 2 is used to verify the accuracy of the methods when dealing with systems that include multiple regions with internal boundary conditions.

3.1. Truncation errors

Leonard (1995) claimed that the CVF is more accurate than the FDM. He made his claim based on expressions he derived for the truncation errors for the two methods. We will derive truncation error expressions for the second and first derivatives for both methods and show that the truncation error expressions are the same for boundary value problems. Consequently, the accuracy of the two methods for this case is the same. We will show that Leonard's expressions for the truncations errors for the CVF are not correct.

The approximation for the first derivative using the FDM is obtained by using Taylor's series expansion for the points ϕ_{j+1} and ϕ_{j-1} about the point ϕ_j.

$$\phi_{j+1} = \phi_j + \Delta X \phi'_j + \frac{\Delta X^2}{2!}\phi''_j + \frac{\Delta X^3}{3!}\phi'''_j + \frac{\Delta X^4}{4!}\phi^{IV}_j + \frac{\Delta X^5}{5!}\phi^{V}_j + \ldots \tag{10}$$

$$\phi_{j-1} = \phi_j - \Delta X \phi_j + \frac{\Delta X^2}{2!}\phi''_j - \frac{\Delta X^3}{3!}\phi'''_j + \frac{\Delta X^4}{4!}\phi^{IV}_j - \frac{\Delta X^5}{5!}\phi^{V}_j + \ldots \tag{11}$$

Subtracting Eqs. (10) and (11).

$$\phi'_j = \frac{\phi_{j+1} - \phi_{j-1}}{2\Delta X} - \frac{\Delta X^2}{6}\phi'''_j - \frac{\Delta X^4}{120}\phi^{V}_j - \ldots \tag{12}$$

Since the first term of the r.h.s. of Eq. (12) is used for the approximation of the first derivative, the truncation error for the first derivative is given by

$$(\text{T.E.})_{1-\text{FDM}} = -\frac{\Delta X^2}{6}\phi'''_j - \frac{\Delta X^4}{120}\phi^{V}_j - \ldots \tag{13}$$

The truncation error for the second derivative using FDM ($(\text{T.E.})_{2-\text{FDM}}$) can be obtained using the same procedure as that for the first derivative. The truncation errors for the first and second derivatives using FDM are summarized in Table 2. When the boundary conditions of the problem involve the first derivative of the variable, a three-point forward or a three-point backward approximation can be used for the left and right boundary, respectively. The approximation for the first derivative at the left boundary is obtained by using Taylor's series expansion for the points ϕ_2 and ϕ_3 about the point ϕ_1. After mathematical manipulation of the series expansions is easy to show that.

$$\left.\frac{d\phi}{dX}\right|_{X=0} = \phi'_{X=0} = \frac{4\phi_2 - \phi_3 - 3\phi_1}{2\Delta X} + \frac{2\Delta X^2}{3!}\phi'''_1 + \frac{6\Delta X^3}{4!}\phi^{IV}_1 + \ldots \tag{14}$$

Taking the first term of the r.h.s. of Eq. (14) for the approximation of the derivative, the truncation error for the first derivative in the left boundary becomes.

$$(\text{T.E.})_{3\text{PF}-\text{FDM}} = \frac{\Delta X^2}{3}\phi'''_1 + \frac{\Delta X^3}{4}\phi^{IV}_1 + \ldots \tag{15}$$

A similar procedure can be used to obtained the truncation error for the right boundary ($(\text{T.E.})_{3\text{PB}-}$ FDM), using a Taylor's series expansion for the points ϕ_{nj-1} and ϕ_{nj-2} about the point ϕ_{nj}. The truncation errors for the left and right boundaries are presented in Table 2.

When using the CVF for a system where the first derivative is involved we get

$$\frac{1}{\Delta X}\int_e^w \frac{d\phi}{dX} dX = \frac{1}{\Delta X}\phi_e - \frac{1}{\Delta X}\phi_w \tag{16}$$

where the ΔX dividing Eq. (16) is obtained from the other terms in the balance that do not involve a derivative of the variable, as we will show later. Values for $(1/\Delta X)\phi_e$ and $(1/\Delta X)\phi_w$ can be obtained by using the PLP or SP profiles (see Eqs. (3)–(6)).

The truncation error for the approximation of the variable at the east face (ϕ_e) using CVF-PLP can be obtained by using Leonard's approach (Leonard, 1994, 1995). His approach consists of using a Taylor's series expansion for the points ϕ_{j+1} and ϕ_j about the point ϕ_e, ϕ_{j-1} about the point ϕ_w, and ϕ_e and ϕ_w about the point ϕ_j.

$$\phi_{j+1} = \phi_e + \frac{\Delta X}{2}\phi'_e + \frac{(\Delta X/2)^2}{2!}\phi''_e + \frac{(\Delta X/2)^3}{3!}\phi'''_e$$

Table 2
Truncation errors of the different models for the derivatives and/or variables using FDM and CVF ($(T.E.)_{V(j)-D(j)}$). $(T.E.)_{V(j)-D(j)}$ represents the truncation error due to the discretisation of the variables and/or derivatives at the volume faces as a function of the node points0

Model of	Method	Error	Equations
$\frac{d\phi}{dX}$ (Left boundary)	FDM	$(T.E.)_{3PF-FDM}=\frac{\Delta X^2}{3}\phi_j'''+\frac{\Delta X^3}{4}\phi_j^{IV}+\ldots$	T2.1
$\frac{d\phi}{dX}$ (Right boundary)	FDM	$(T.E.)_{3PB-FDM}=\frac{\Delta X^2}{3}\phi_j'''-\frac{\Delta X^3}{4}\phi_j^{IV}+\ldots$	T2.2
$\frac{d\phi}{dX}$ (Governing equation)	FDM	$(T.E.)_{1-FDM}=-\frac{\Delta X^2}{6}\phi_j'''-\frac{\Delta X^4}{120}\phi_j^{V}-\ldots$	T2.3
$\frac{d^2\phi}{dX^2}$ (Governing equation)	FDM	$(T.E.)_{2-FDM}=-\frac{\Delta X^2}{12}\phi_j^{IV}-\frac{\Delta X^4}{360}\phi_j^{VI}-\ldots$	T2.4
$\frac{1}{\Delta X}\frac{d\phi}{dX}\Big\|_e$	CVF-PLP	$(T.E)_{e-PLP,1}=-\frac{\Delta X}{24}\phi_j'''-\frac{\Delta X^2}{48}\phi_j^{IV}-11\frac{\Delta X^3}{1920}\phi_j^{V}-13\frac{\Delta X^4}{11520}\phi_j^{VI}-\ldots$	T2.5[a]
$\frac{1}{\Delta X}\frac{d\phi}{dX}\Big\|_w$	CVF-PLP	$(T.E.)_{w-PLP,1}=-\frac{\Delta X}{24}\phi_j'''+\frac{\Delta X^2}{48}\phi_j^{IV}-11\frac{\Delta X^3}{1920}\phi_j^{V}+13\frac{\Delta X^4}{11520}\phi_j^{VI}-\ldots$	T2.6[a]
$\frac{1}{\Delta X}\frac{d\phi}{dX}\Big\|_e-\frac{1}{\Delta X}\frac{d\phi}{dX}\Big\|_w$	CVF-PLP	$(T.E.)_{e-w,PLP-1}=-\frac{\Delta X^2}{24}\phi_j^{IV}-13\frac{\Delta X^4}{5760}\phi_j^{VI}-\ldots$	T2.7[a]
$\frac{\phi_e}{\Delta X}$	CVF-PLP	$(T.E)_{e-PLP,V}=-\frac{\Delta X}{8}\phi_j'''-\frac{\Delta X^2}{16}\phi_j'''-7\frac{\Delta X^3}{384}\phi_j^{IV}-\frac{\Delta X^4}{256}\phi_j^{V}-\ldots$	T2.8[a]
$\frac{\phi_w}{\Delta X}$	CVF-PLP	$(T.E.)_{w-PLP,V}=-\frac{\Delta X}{8}\phi_j''+\frac{\Delta X^2}{16}\phi_j'''-7\frac{\Delta X^3}{384}\phi_j^{IV}+\frac{\Delta X^4}{256}\phi_j^{V}-\ldots$	T2.9[a]
$\frac{\phi_e}{\Delta X}-\frac{\phi_w}{\Delta X}$	CVF-PLP	$(T.E.)_{e-w,PLP-V}=-\frac{\Delta X^2}{8}\phi_j'''-\frac{\Delta X^4}{128}\phi_j^{V}-\ldots$	T2.10[a]
$\frac{\phi_e}{\Delta X}$	CVF-SP	$(T.E.)_{e-SP}=\frac{\phi_j'}{2}+\frac{\Delta X}{8}\phi_j''+\frac{\Delta X^2}{48}\phi_j'''+\frac{\Delta X^3}{384}\phi_j^{IV}+\ldots$	T2.11[a]
$\frac{\phi_w}{\Delta X}$	CVF-SP	$(T.E.)_{w-SP}=\frac{\phi_j'}{2}-3\frac{\Delta X}{8}\phi_j''+7\frac{\Delta X^2}{48}\phi_j'''-5\frac{\Delta X^3}{128}\phi_j^{IV}+\ldots$	T2.12[a]
$\frac{\phi_e}{\Delta X}-\frac{\phi_w}{\Delta X}$	CVF-SP	$(T.E.)_{e-w,SP}=\frac{\Delta X}{2}\phi_j''-\frac{\Delta X^2}{8}\phi_j'''+\frac{\Delta X^3}{24}\phi_j^{IV}+\ldots$	T2.13[a]

[a] Represents $(T.E.)7_{V(j)-D(j)}$.

$$+\frac{(\Delta X/2)^4}{4!}\phi_e^{IV}+\frac{(\Delta X/2)^5}{5!}\phi_e^{V}+\ldots \quad (17)$$

$$\phi_j=\phi_e-\frac{\Delta X}{2}\phi_e'+\frac{(\Delta X/2)^2}{2!}\phi_e''-\frac{(\Delta X/2)^3}{3!}\phi_e'''+\frac{(\Delta X/2)^4}{4!}\phi_e^{IV}-\frac{(\Delta X/2)^5}{5!}\phi_e^{V}+\ldots \quad (18)$$

$$\phi_j=\phi_w+\frac{\Delta X}{2}\phi_w'+\frac{(\Delta X/2)^2}{2!}\phi_w''+\frac{(\Delta X/2)^3}{3!}\phi_w'''+\frac{(\Delta X/2)^4}{4!}\phi_w^{IV}+\frac{(\Delta X/2)^5}{5!}\phi_w^{V}+\ldots \quad (19)$$

$$\phi_{j-1}=\phi_w-\frac{\Delta X}{2}\phi_w'+\frac{(\Delta X/2)^2}{2!}\phi_w''-\frac{(\Delta X/2)^3}{3!}\phi_w'''+\frac{(\Delta X/2)^4}{4!}\phi_w^{IV}-\frac{(\Delta X/2)^5}{5!}\phi_w^{V}+\ldots \quad (20)$$

$$\phi_e=\phi_j+\frac{\Delta X}{2}\phi_j'+\frac{(\Delta X/2)^2}{2!}\phi_j''+\frac{(\Delta X/2)^3}{3!}\phi_j'''+\frac{(\Delta X/2)^4}{4!}\phi_j^{IV}+\frac{(\Delta X/2)^5}{5!}\phi_j^{V}+\ldots \quad (21)$$

$$\phi_w=\phi_j-\frac{\Delta X}{2}\phi_j'+\frac{(\Delta X/2)^2}{2!}\phi_j''-\frac{(\Delta X/2)^3}{3!}\phi_j'''+\frac{(\Delta X/2)^4}{4!}\phi_j^{IV}-\frac{(\Delta X/2)^5}{5!}\phi_j^{V}+\ldots \quad (22)$$

Adding Eqs. (17)–(20) yields

$$\phi_e=\frac{(\phi_{j+1}+\phi_j)}{2}-\frac{\Delta X^2}{8}\phi_e''-\frac{\Delta X^4}{384}\phi_e^{IV}-\ldots \quad (23)$$

$$\phi_w=\frac{(\phi_j+\phi_{j-1})}{2}-\frac{\Delta X^2}{8}\phi_w''-\frac{\Delta X^4}{384}\phi_w^{IV}-\ldots \quad (24)$$

Taking the derivatives of Eq. (21) respect to X (second and fourth derivatives), substituting into Eq. (23) and dividing the expression by ΔX yields.

$$\frac{\phi_e}{\Delta X}=\frac{(\phi_{j+1}+\phi_j)}{2\Delta X}-\frac{\Delta X}{8}\phi_j''-\frac{\Delta X^2}{16}\phi_j'''-\ldots \quad (25)$$

Taking the first term of the r.h.s of Eq. (25) as the approximation for the variable at the east face, the error for this approximation using CVF-PLP ($(T.E.)_{e-PLP,V}$) becomes

$$(\text{T.E.})_{e-\text{PLP,V}} = -\frac{\Delta X}{8}\phi_j'' - \frac{\Delta X^2}{16}\phi_j''' - 7\frac{\Delta X^3}{384}\phi_j^{IV} - \frac{\Delta X^4}{256}\phi_j^{V} - \ldots \quad (26)$$

The truncation error for the approximation of the variable at the west face using CVF-PLP ($(\text{T.E.})_{w-\text{PLP,V}}$) can be obtained by taking the derivatives of Eq. (22) respect to X (second and fourth derivatives), substituting into Eq. (24) and dividing the expression by ΔX. The equations for the truncation errors of the variables using CVF-PLP are given in Table 2.

A similar procedure can be used to obtain the truncation error for the approximations of the variable at the east and west faces using CVF-SP ($(\text{T.E.})_{e-\text{SP}}$ and $(\text{T.E.})_{w-\text{SP}}$, respectively). Also, Leonard's approach can be extended to obtain the truncation errors for the approximation of the first derivative at the east and west faces using CVF $(\text{T.E.})_{e-\text{PLP,1}}$ and $(\text{T.E.})_{w-\text{PLP,1}}$). All these equations are summarized in Table 2.

According to the approximations obtained for the variables evaluated at the east and west faces (Eqs. (23) and (24)) Eq. (16) becomes:

$$\frac{1}{\Delta X}\int_e^w \frac{d\phi}{dX}\,dX = \frac{1}{\Delta X}\phi_e - \frac{1}{\Delta X}\phi_w = \frac{\phi_{j+1} - \phi_{j-1}}{2\,\Delta X} + (\text{T.E.})_{e-w,\text{PLP-V}} \quad (27)$$

where the truncation error for the approximation of the variable at the east face minus the approximation of the variable at the west face using CVF-PLP ($(\text{T.E.})_{e-w,\text{PLP}-\text{V}}$) is obtained by subtracting Eq. T2.9 from Eq. T2.8:

$$(\text{T.E.})_{e-w,\text{PLP-V}} = -\frac{\Delta X^2}{8}\phi_j''' - \frac{\Delta X^4}{128}\phi_j^{V} - \ldots \quad (28)$$

Since Leonard stated that Eq. (16) is exact (Leonard, 1995), the truncation error for the approximation of the variable at the east face minus the approximation of the variable at the west face represents the truncation error of the CVF-PLP method:

$$(\text{T.E.})_{\text{CVF-PLP}} = (\text{T.E.})_{e-w,\text{PLP-V}} \quad (29)$$

The first term of the r.h.s. of Eq. (12) represents the discretised equation for the first derivative used in the FDM (Eq. T1.3), while the first term of the r.h.s. of Eq. (27) is the expression used for the first derivative in the CVF-PLP (Eq. T1.10). As one can see both terms are the same (Eqs. T1.3 and T1.10 in Table 1); therefore, for fixed boundary node values the FDM and the CVF-PLP will yield to the same solution. Since both methods yield to the same expression for the first derivative, their accuracy and their truncation errors must be the same. However, according to the truncation errors, the CVF-PLP (see Eqs. (28) and (29)) will be more accurate than the FDM (see Eq. (13)). It is important to know that this conclusion is not correct and both truncation errors should be the same. The inconsistency in the truncation errors is due to the fact that Eq. (16) represents the exact solution at the volume faces but not at the node points needed.

This same problem exists for Leonard's truncation error expression for the second derivative. This can be seen by subtracting Eq. T2.6 from Eq. T2.5 which yields (compare to Eq. A-60 in Leonard, 1995).

$$(\text{T.E.})_{\text{CVF-PLP}} = -\frac{\Delta X^2}{24}\phi_j^{IV} - \frac{13}{5760}\Delta X^4\,\phi_j^{VI} \quad (30)$$

According to Eq. (30) the truncation error for the solution of a second order differential equation using CVF-PLP is smaller than the truncation error using FDM (see Eq. T2.4), which is not true as we explain next. The equations for the approximation associated with Eq. (30) are.

$$\frac{1}{\Delta X}\int_w^e \frac{d^2\phi}{dX^2}\,dX = \frac{1}{\Delta X}\left(\frac{d\phi}{dX}\Big|_e - \frac{d\phi}{dX}\Big|_w\right) = \frac{\phi_{j+1} - 2\phi_j + \phi_{j-1}}{\Delta X^2} \quad (31)$$

Eq. (31) yields the same approximation that the FDM yields for the second derivative evaluated at the node '*j*' (see Eq. T1.4). Note that the approximations for the solution of a second order differential equation using both methods are the same (compare Eqs. T1.4 and T1.7). Since the equations for the approximations are the same, the truncation errors must be the same. The truncation error represented by Eq. (30) includes the truncation errors associated with expressing the first derivatives at the east and west faces as a function of the nodes j, $j+1$, and $j-1$. That is, Eq. (30) contains only the truncation errors for the derivatives evaluated at the faces of the control volume. However, the solution of the problem is required at the node points and not at the faces of the control volume; therefore the truncation error of interest is that associated with the node points. To determine this truncation error, the approximation that the CVF method uses for the integral of the variable over the control volume formulation will be used (generally used for representing source terms in the balances). According to the CVF the integration of the variable over the control volume is approximated by (Patankar, 1980; Leonard, 1995):

$$\int_w^e \phi\,dX \approx \phi_j \Delta X \quad (32)$$

where it is assumed that the value of the dependent variable evaluated at node point 'j' times ΔX is equal to the integral of the variable from 'w' to 'e'. This assumption is true because the mean-value theorem for integral calculus states that if a function is continuous on the closed interval [w, e], there is a number ξ, with $w \le \xi \le e$, such that.

$$\int_w^e \phi \, dX = \phi(\xi)\Delta X \tag{33}$$

Choosing $\xi = X_j$ is an approximation. By analogy with Eq. (32) the integral of the second derivative over the control volume followed by applying the mean-value theorem of integral calculus yields.

$$\int_w^e \frac{d^2\phi}{dX^2} dX = \phi_j'' \, \Delta X \tag{34}$$

Again, the evaluation of ϕ'' at X_j and not at ξ is an approximation. An approximation for ϕ_j'' can be obtained by taking the derivatives of Eqs. (21) and (22) respect to X, subtracting the results and rearranging.

$$\phi_j'' = \frac{1}{\Delta X}(\phi_e' - \phi_w') - \frac{\Delta X^2}{24}\phi_j^{IV} - \frac{\Delta X^4}{1920}\phi_j^{VI} - \ldots \tag{35}$$

Eq. (35) shows the differences between the second derivative evaluated at the node point and the gradient of the first derivative between the east and west faces of the control volume. This equation indicates that evaluating the difference of the first derivatives at the east and west faces should over-predict the results obtain by evaluating the second derivative at the node point.

Substituting Eq. (35) into Eq. (34) followed by rearrangement yields:

$$\frac{1}{\Delta X}\int_w^e \frac{d^2\phi}{dX^2} dX = \frac{1}{\Delta X}\left(\frac{d\phi}{dX}\Big|_e - \frac{d\phi}{dX}\Big|_w\right) + (T.E.)_{D-e,w\to j} \tag{36}$$

where $(T.E.)_{D-e,w\to j}$ represents the truncation error associated with the derivatives evaluated at the faces of the control volume (east and west), and it is given by.

$$(T.E.)_{D-e,w\to j} = -\frac{\Delta X^2}{24}\phi_j^{IV} - \frac{\Delta X^4}{1920}\phi_j^{VI} - \ldots \tag{37}$$

Finally, the truncation error for the approximation of the second derivative using CVF-PLP can be obtained by adding Eqs. (37) and (30) which yields:

$$(T.E.)_{CVF\text{-}PLP} = -\frac{\Delta X^2}{12}\phi_j^{IV} - \frac{\Delta X^4}{360}\phi_j^{VI} - \ldots \tag{38}$$

which is the same as the truncation error for the second derivative using FDM (see Table 2, Eq. T2.4).

To demonstrate the validity of Eq. (38) and that Eq. (30) is wrong, consider the following simple system. A rectangular bar enclosed in a vacuum environment with a heat consumption source. The governing equation is

$$\frac{d^2T}{dX^2} = b_1 T \tag{39}$$

where b_1 is a dimensionless parameter. To eliminate the effect of the truncation errors of the boundary conditions, we assume that the boundary temperatures are known:

$$T = T_{left} \text{ at } X = 0 \tag{40}$$

$$T = T_{right} \text{ at } X = 1 \tag{41}$$

The analytical solution is given by:

$$T = \frac{[T_{right} - T_{left}\cosh\sqrt{b_1}]}{\sinh\sqrt{b_1}}\sinh(\sqrt{b_1}X) + T_{left}\cosh(\sqrt{b_1}X) \tag{42}$$

The discretised equations for Eq. (39) using the FDM and CVF in this case are the same; therefore the numerical solution obtained by the two methods will be the same. The equations were solved for 6 nodes (nj = 6). We developed a technique that allows calculating the values of the truncation errors from the numerical solution when the analytical solution is known. Details for the derivation of this technique are given in the Appendix A. The advantage of the technique is that it allows: 1. Calculating the total truncation error, 2. Calculating and evaluating the effect of the round-off errors, and 3. Verifying the values obtained for the theoretical truncation errors, i.e. using Taylor's series expansion. The discretised equations were solved using Maple V and the truncation errors were calculated using the technique proposed in the Appendix A. Some important results are summarized below for $b_1 = 1$, $T_{left} = 350°C$, and $T_{right} = 200°C$:

$$\mathbf{T} = \begin{pmatrix} 350.000 \\ 298.761 \\ 259.512 \\ 230.679 \\ 211.103 \\ 200.000 \end{pmatrix} \qquad \mathbf{T}_{FDM\text{-}CVF} = \begin{pmatrix} 350.000 \\ 298.826 \\ 259.604 \\ 230.767 \\ 211.160 \\ 200.000 \end{pmatrix}$$

$$\mathbf{TE} = \begin{pmatrix} 0.000 \\ -0.997 \\ -0.866 \\ -0.769 \\ -0.707 \\ 0.000 \end{pmatrix} \qquad (\mathbf{T.E.})_{FDM} = \begin{pmatrix} 0.000 \\ -0.997 \\ -0.866 \\ -0.769 \\ -0.705 \\ 0.000 \end{pmatrix}$$

$$(\mathbf{T.E.})_{CVF\text{-}PLP\ (Eq.30)} = \begin{pmatrix} 0.000 \\ -0.499 \\ -0.433 \\ -0.385 \\ -0.352 \\ 0.000 \end{pmatrix}$$

where $\mathbf{T}$, $\mathbf{T}_{FDM\text{-}CVF}$, $\mathbf{TE}$, $(\mathbf{T.E.})_{FDM}$, and $(\mathbf{T.E.})_{CVF\text{-}PLP(Eq.\ (30))}$, represent the analytical solution vector,

the numerical solution vector, the truncation error vector calculated from the numerical solution, the truncation error vector for the FDM calculated from Eq. T2.4, and the truncation error vector predicted by using Leonard's approach (i.e. calculated from Eq. (30)), respectively. The truncation errors predicted by Eq. T2.4 which is the same as Eq. (38) match well the truncation errors obtained from the numerical solution (compare **TE** to $(\mathbf{T.E.})_{FDM}$). As expected, the truncation errors predicted by Leonard's approach (Eq. (30)) do not agree with the calculated truncation errors (compare **TE** to $(\mathbf{T.E.})_{CVF\text{-}PLP(}$Eq. (30)$_)$. Again, the calculated truncation errors (**TE**) agree well with the predicted truncation errors obtained from Eq. (38), which is the same equation as T2.4), and disagree significantly with those predicted by Leonard's Eq. (30). This shows clearly that the truncation errors are the same for the two methods (FDM and CVF). The truncation error for the CVF method is not smaller than that for the FDM as claimed by Leonard. Note that Eq. (38) can be obtained by adding Eq. T3.2 to Eq. (30).

Truncation errors for other equations using the CVF can be calculated by

$$(\text{T.E.})_{CVF} = (\text{T.E.})_{V(j)-D(j)} + (\text{T.E.})_{V,D\to j} \tag{43}$$

where the first term in the r.h.s. of Eq. (43) represents the truncation error associated with expressing the variables and/or the derivatives as a function of the node points (discretisation), and the second term represents the truncation error caused by solving the algebraic equations at the node points and not at the volume faces. Expressions for $(\text{T.E.})_{V(j)-D(j)}$ are given in Table 2 and typical expressions for $(\text{T.E.})_{V,D\to j}$ are presented in Table 3. For instance, to calculate the truncation error of $1/\Delta X \int_w^e d\phi/dX \times dX = 1/\Delta X(\phi|_e - \phi|_w)$ using PLP, Eqs. T2.10 ($(\text{T.E.})_{V(j)-D(j)}$) and T3.1 ($(\text{T.E.})_{V,D\to j}$) should be added; therefore the total truncation error for this case would be.

Table 3
Truncation error in the CVF caused by solving the algebraic equations at the node points and not at the volume faces ($(\text{T.E.})_{V,D\to j}$)

Used for	$(\text{T.E.})_{V,D\to j}$	Equations
$\frac{1}{\Delta X}\int_w^e \frac{d\phi}{dX}dX = \frac{1}{\Delta X}(\phi_e - \phi_w)$	$(\text{T.E.})_{V-e,w\to j} = -\frac{\Delta X^2}{24}\phi_j''' - \frac{\Delta X^4}{1920}\phi_j^V - \ldots$	T3.1
$\frac{1}{\Delta X}\int_w^e \frac{d^2\phi}{dX^2}dX = \frac{1}{\Delta X}\left(\frac{d\phi}{dX}\Big\|_e - \frac{d\phi}{dX}\Big\|_w\right)$	$(\text{T.E.})_{D-e,w\to j} = -\frac{\Delta X^2}{24}\phi_j^{IV} - \frac{\Delta X^4}{1920}\phi_j^{VI} - \ldots$	T3.2
$\frac{2}{\Delta X}\int_{B_l}^{ii_l} \frac{d\phi}{dX}dX = \frac{2}{\Delta X}(\phi_{ii_l} - \phi_{B_l})$	$(\text{T.E.})_{V-l\to j} = -\frac{\Delta X^2}{96}\phi_j''' - \frac{\Delta X^3}{384}\phi_j^{IV} - \frac{\Delta X^4}{3072}\phi_j^V - \ldots$	T3.3*
$\frac{2}{\Delta X}\int_{ii_r}^{B_r} \frac{d\phi}{dX}dX = \frac{2}{\Delta X}(\phi_{B_r} - \phi_{ii_r})$	$(\text{T.E.})_{V-r\to j} = -\frac{\Delta X^2}{96}\phi_j''' + \frac{\Delta X^3}{384}\phi_j^{IV} - \frac{\Delta X^4}{3072}\phi_j^V + \ldots$	T3.4**
$\frac{2}{\Delta X}\int_{B_l}^{ii_l} \frac{d^2\phi}{dX^2}dX = \frac{2}{\Delta X}\left(\frac{d\phi}{dX}\Big\|_{ii_l} - \frac{d\phi}{dX}\Big\|_{B_l}\right)$	$(\text{T.E.})_{D-l\to j} = -\frac{\Delta X^2}{96}\phi_j^{IV} - \frac{\Delta X^3}{384}\phi_j^V - \frac{\Delta X^4}{3072}\phi_j^{VI} - \ldots$	T3.5*
$\frac{2}{\Delta X}\int_{ii_r}^{B_r} \frac{d^2\phi}{dX^2}dX = \frac{2}{\Delta X}\left(\frac{d\phi}{dX}\Big\|_{B_r} - \frac{d\phi}{dX}\Big\|_{ii_r}\right)$	$(\text{T.E.})_{D-r\to j} = -\frac{\Delta X^2}{96}\phi_j^{IV} + \frac{\Delta X^3}{384}\phi_j^V - \frac{\Delta X^4}{3072}\phi_j^{VI} + \ldots$	T3.6**
$\frac{\phi_e + \phi_w}{2}$	$(\text{T.E.})_{V,e+w\to j} = -\frac{\Delta X^2}{8}\phi_j'' - \frac{\Delta X^4}{384}\phi_j^{IV} - \ldots$	T3.7
$\frac{1}{2}\left(\frac{d\phi}{dX}\Big\|_e + \frac{d\phi}{dX}\Big\|_w\right)$	$(\text{T.E.})_{D,e+w\to j} = -\frac{\Delta X^2}{8}\phi_j''' - \frac{\Delta X^4}{384}\phi_j^V - \ldots$	T3.8
$\frac{\phi_{B_r} + \phi_{ii_r}}{2}$	$(\text{T.E.})_{V,B_r+ii_r\to j} = -\frac{\Delta X^2}{32}\phi_j'' + \frac{\Delta X^3}{128}\phi_j''' - \ldots$	T3.9*
$\frac{\phi_{B_l} + \phi_{ii_l}}{2}$	$(\text{T.E.})_{V,B_l+ii_l\to j} = -\frac{\Delta X^2}{32}\phi_j'' - \frac{\Delta X^3}{128}\phi_j''' - \ldots$	T3.10**
$\frac{1}{2}\left(\frac{d\phi}{dX}\Big\|_{B_r} + \frac{d\phi}{dX}\Big\|_{ii_r}\right)$	$(\text{T.E.})_{D,B_r+ii_r\to j} = -\frac{\Delta X^2}{32}\phi_j''' + \frac{\Delta X^3}{128}\phi_j^{IV} - \ldots$	T3.11*
$\frac{1}{2}\left(\frac{d\phi}{dX}\Big\|_{B_l} + \frac{d\phi}{dX}\Big\|_{ii_l}\right)$	$(\text{T.E.})_{D,B_l+ii_l\to j} = -\frac{\Delta X^2}{32}\phi_j''' - \frac{\Delta X^3}{128}\phi_j^{IV} - \ldots$	T3.12**
$\frac{2}{\Delta X}\int_{B_l}^{ii_l}\phi\,dX = \phi_l$	$(\text{T.E.})_{\nabla-l\to 1} = \frac{\Delta X}{4}\phi_1' + \frac{\Delta X^2}{32}\phi_1'' + \frac{\Delta X^3}{384}\phi_1''' + \ldots$	T3.13*
$\frac{2}{\Delta X}\int_{ii_r}^{B_r}\phi\,dX = \phi_r$	$(\text{T.E.})_{\nabla-r\to nj} = -\frac{\Delta X}{4}\phi_{nj}' + \frac{\Delta X^2}{32}\phi_{nj}'' - \frac{\Delta X^3}{384}\phi_{nj}''' + \ldots$	T3.14**

* Approximate value, the value is assumed to be located at $1+1/4$ ($\xi = X_1 + \Delta X/4$)).
** Approximate value, the value is assumed to be located at $nj-1/4$ ($\xi = X_{nj} - \Delta X/4$)).

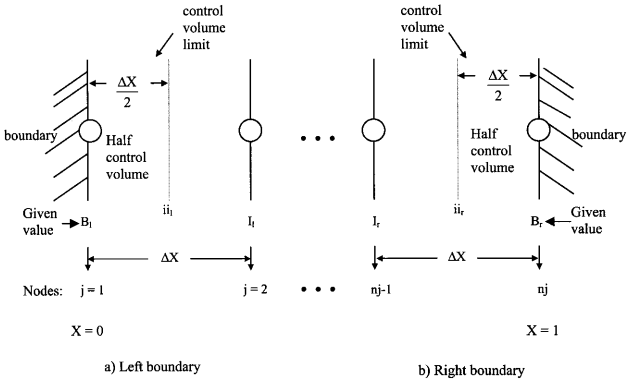

Fig. 3. Treatment of the boundary conditions in example 1 using the control volume formulation.

$$(\text{T.E.})_{\text{CVF-PLP}} = -\frac{\Delta X^2}{6}\phi_j''' - \frac{\Delta X^4}{120}\phi_j^{V} - \ldots \tag{44}$$

Eq. (44) is the same as the truncation error for the first derivative using FDM (see Eq. T2.3). The values for $(\text{T.E.})_{V,D\to j}$ will depend on the case study; the equations shown in Table 3 can be used as a basis from which to derive other cases. For example, the procedure to calculate the truncation error for CVF in cylindrical coordinates is given next. The equation for the central nodes in cylindrical coordinates is given by:

$$\frac{1}{\Delta X}\int_w^e \frac{d}{dX}\left(X\frac{d\phi}{dX}\right)dX = \frac{1}{\Delta X}\left(X_e\frac{d\phi}{dX}\Big|_e - X_w\frac{d\phi}{dX}\Big|_w\right) \tag{45}$$

where $X_e = X_j + (\Delta X/2)$ and $X_w = X_j + (\Delta X/2)$. Eq. (45) is not directly represented in Table 3; however, it can be rearranged to use the expressions given in Table 3. Substituting X_e and X_w into Eq. (45) and rearranging.

$$\frac{1}{\Delta X}\left(X_e\frac{d\phi}{dX}\Big|_e - X_w\frac{d\phi}{dX}\Big|_w\right) = \frac{X_j}{\Delta X}\left(\frac{d\phi}{dX}\Big|_e - \frac{d\phi}{dX}\Big|_w\right) + \frac{1}{2}\left(\frac{d\phi}{dX}\Big|_e + \frac{d\phi}{dX}\Big|_w\right) \tag{46}$$

The error associated with the first term on the r.h.s. of Eq. (46) is given by Eq. T3.2 (Table 3) while the error for the second term is given by Eq. T3.8, therefore:

$$\frac{1}{\Delta X}\int_w^e \frac{d}{dX}\left(X\frac{d\phi}{dX}\right)dX = \frac{1}{\Delta X}\left(X_e\frac{d\phi}{dX}\Big|_e - X_w\frac{d\phi}{dX}\Big|_w\right) + (\text{T.E.})_{\text{Cyl}-e,w\to j} \tag{47}$$

where the truncation error associated with the approximation of the derivative evaluated at the node *j* by the derivatives evaluated at the faces of the control volume for cylindrical coordinates is given by.

$$(\text{T.E.})_{\text{Cyl}-e,w\to j} = -\frac{\Delta X^2}{8}\left(\phi_j''' + \frac{X_j}{3}\phi_j^{IV}\right) - \frac{\Delta X^4}{384}\left(\phi_j^{V} + \frac{X_j}{5}\phi_j^{VI}\right) - \ldots \tag{48}$$

3.1.1. Boundary conditions

The solution of the problem will depend on the boundary conditions; therefore, in order to complete the analysis of truncation errors of a problem, the truncation errors of the approximations used for the boundary conditions should be included. We can have three different kinds of boundary conditions: Dirichlet, in which the value of the variable is given; Neumann, in which the value of the first derivative is known; and Robin that is a combination of Dirichlet and Neumann boundary conditions. Knowing this, we can have different combinations at the two boundaries (1) Dirichlet at both boundaries, (2) Dirichlet at one boundary and Neumann at the other, (3) Robin at one boundary and Dirichlet at the other, and (4) Robin at both boundaries, and (5) Neumann at both boundaries. It is worth noting that Neumann conditions at both boundaries cannot be solved for a steady state problem because infinite many solutions exist for such a case.

When both boundary conditions are of the Dirichlet kind, the error of the approximation of the system is defined by the error of the approximations used in the governing equation as we have shown above. The truncation errors for other kinds of boundary conditions using FDM can be obtained from Table 2.

The truncation errors at the boundaries using CVF method need to be derived. The methodology explained above can be used to determine the truncation errors associated with the boundary conditions for the CVF method by applying the mean-value theorem of integral calculus at the middle point of half of a control volume. This assumption is based on the methodology used by the CVF to treat source terms as shown in Eq. (32). According to Eq. (32) the variable is evaluated at the 'j' node that corresponds with the center of the control volume for the central control volumes (see Fig. 1b). In the same way, when applying the mean-value theorem of integral calculus at the boundaries, the variable should be evaluated at the center of the control volume, that is at $X = \Delta X/4$ for the left boundary (see Fig. 3a) and $X = 1 - (\Delta X/4)$ for the right boundary (see Fig. 3b). For example, consider applying the mean value theorem for the second derivative of the variable over the half control volume shown in Fig. 3b (at $X = 1$):

$$\int_{ii_r}^{B_r}\frac{d^2\phi}{dX^2}dX = \phi''_{nj-1/4}\frac{\Delta X}{2} \tag{49}$$

where ϕ'' is evaluated at the center of the half control volume. Eq. (49) is an approximation where $\xi = X_j - (\Delta X/4)$ (i.e. $nj - 1/4$) was assumed. Expanding ϕ_{B_r} and ϕ_{ii_r} about $\phi_{nj-1/4}$ using Taylor's series expansions yields.

$$\phi_{B_r} = \phi_{nj-1/4} + \frac{\Delta X}{4}\phi'_{nj-1/4} + \frac{(\Delta X/4)^2}{2!}\phi''_{nj-1/4} + \frac{(\Delta X/4)^3}{3!}\phi'''_{nj-1/4} + \frac{(\Delta X/4)^4}{4!}\phi^{IV}_{nj-1/4} + \ldots \tag{50}$$

$$\phi_{ii_r} = \phi_{nj-1/4} - \frac{\Delta X}{4}\phi'_{nj-1/4} + \frac{(\Delta X/4)^2}{2!}\phi''_{nj-1/4} - \frac{(\Delta X/4)^3}{3!}\phi'''_{nj-1/4} + \frac{(\Delta X/4)^4}{4!}\phi^{IV}_{nj-1/4} - \ldots \quad (51)$$

Subtracting Eq. (51) from Eq. (50) and rearranging yields.

$$\phi''_{nj-1/4} = 2\frac{(\phi'_{B_r} - \phi'_{ii_r})}{\Delta X} - \frac{\Delta X^2}{96}\phi^{IV}_{nj-1/4} - \ldots \quad (52)$$

Expanding $\phi_{nj-1/4}$ about ϕ_{nj} and taking the required derivatives of the expansion with respect to X, gives

$$\phi^{IV}_{nj-1/4} = \phi^{IV}_{nj} - \frac{\Delta X}{4}\phi^{V}_{nj} + \frac{\Delta X^2}{32}\phi^{VI}_{nj} - \frac{\Delta X^3}{384}\phi^{VII}_{nj} + \ldots \quad (53)$$

Substituting Eqs. (53) and (52) into Eq. (49) and rearranging yields:

$$\frac{2}{dX}\int_{ii_r}^{B_r}\frac{d^2\phi}{dX^2}dX = 2\frac{(\phi'_{B_r} - \phi'_{ii_r})}{\Delta X} + (T.E.)_{D-r\to nj} \quad (54)$$

where the error associated with evaluating the variable at the middle point of the half control volume is given by.

$$(T.E.)_{D-r\to nj} = -\frac{\Delta X^2}{96}\phi^{IV}_{nj} + \frac{\Delta X^3}{384}\phi^{V}_{nj} - \frac{\Delta X^4}{3072}\phi^{VI}_{nj} + \ldots \quad (55)$$

Using the same procedure, truncation errors related to the variables in the boundary conditions can be calculated, these errors are summarized in Table 3 (Eqs. T3.13 and T3.14 for the left and right boundary, respectively).

In order to illustrate how to analyze the accuracy of the methods including the boundary conditions a simple problem is solved. Consider a rectangular fin as described by Davis (1984). The equations that describe this system are given by:

$$\frac{d^2T}{dX^2} = H^2(T - T_a) \quad (56)$$

$$T = T_{left} \text{ at } X = 0 \quad (57)$$

$$\frac{dT}{dX} = 0 \text{ at } X = 1 \quad (58)$$

where H is a parameter, and T_a is the ambient temperature. The discretised equations for this system are:

$$* \quad \text{for } 2 < j < nj: \frac{\phi_{j+1} - 2\phi_j + \phi_{j-1}}{\Delta X^2} = H^2(\phi_j - T_a) \text{ for the FDM and CVF} \quad (59)$$

$$* \quad j = nj: \frac{3\phi_{nj} - 4\phi_{nj-1} + \phi_{nj-2}}{2\Delta X} = 0 \text{ for the FDM} \quad (60)$$

To obtain the discretised equation for the right boundary using the CVF-PLP method, Eq. (56) needs to be integrated over the half of control volume shown in Fig. 3b:

$$\int_{ii_r}^{B_r}\frac{d^2T}{dX^2}dX = \int_{ii_r}^{B_r} H^2(T - T_a)dX \quad (61)$$

then

$$\frac{dT}{dX}\Big|_{B_r} - \frac{dT}{dX}\Big|_{ii_r} = H^2(\overline{T} - T_a)\frac{\Delta X}{2} \quad (62)$$

where $\bar{T}$ is the control volume average temperature. The derivative of the temperature at the right boundary is known ($dT/dX|_{B_r} = 0$ from boundary condition Eq. (58)). The first derivative at the internal interface (ii_r) and the control volume average temperature need to be discretised. The PLP profile is used to discretise the derivative evaluated at the internal interface (see Eq. T1.6) and the control volume average temperature is approximated with the variable evaluated at the node point 'nj'. The discretised equation for the right boundary using CVF-PLP represented with the discretised variable ϕ is given by.

$$-\frac{2(\phi_{nj} - \phi_{nj-1})}{\Delta X^2} = H^2(\phi_{nj} - T_a) \quad (63)$$

The truncation errors for the central nodes for both methods (CVF and FDM) are the same for this case, and they are given by.

$$(T.E.)_{FDM} = (T.E.)_{CVF\text{-}PLP} = -\frac{\Delta X^2}{12}\phi^{IV}_j - \frac{\Delta X^4}{360}\phi^{VI}_j - \ldots \quad \text{for central nodes} \quad (64)$$

Therefore, the differences in the solutions between the two methods depend on the approximations used and the truncation errors for the right boundary. The truncation errors for the right boundary are given by.

$$(T.E.)_{3PB\text{-}FDM} = \frac{\Delta X^2}{3}\phi'''_j - \frac{\Delta X^3}{4}\phi^{IV}_j + \ldots \quad \text{for the FDM} \quad (65)$$

The total truncation error for Eq. (63) (using CVF-PLP) can be obtained by subtracting two times Eq. T2.6 from Eq. (55). As it was mentioned before the control volume average temperature was approximated with the temperature evaluated at the node point nj, therefore, the error associated with this approximation should also be incorporated in the total truncation error. The truncation error for the average of the variable ($(T.E.)_{\overline{V}-r\to j}$) is given by Eq. T3.14. Therefore the total truncation error associated with Eq. (63) (using CVF-PLP) is given by.

$$(T.E.)_{CVF\text{-}PLP} = -2(T.E.)_{w-PLP,1} + (T.E.)_{D-r\to j} - H^2(T.E.)_{\overline{V}-r\to j} \quad (66)$$

Thus,

$$(\text{T.E.})_{\text{CVF-PLP}} = \frac{\Delta X}{12}\phi_j''' - \frac{\Delta X^2}{24}\phi_j^{IV} + 11\frac{\Delta X^3}{960}\phi_j^{V} - \frac{\Delta X^2}{96}\phi_j^{IV} + \frac{\Delta X^3}{384}\phi_j^{V} - H^2\left(-\frac{\Delta X}{4}\phi_j' + \frac{\Delta X^2}{32}\phi_j'' - \frac{\Delta X^3}{384}\phi_j'''\right) \quad (67)$$

The truncation error for the right boundary condition using FDM is order $(\Delta X)^2$ (see Eq. (65)), while the truncation error for the CVF-PLP is order (ΔX) (see Eq. (67)). In addition, the truncation error for the CVF-PLP right boundary is a direct function of the dimensionless parameter H, while for the FDM is only an indirect function through the derivatives of the variable.

The analytical solution for Eqs. (56)–(58) is given by:

$$T = T_a + \frac{(T_{left} - T_a)\cosh[H(1-X)]}{\cosh(H)} \quad (68)$$

The discretised equations were solved using Maple. The solution was obtained for $T_a = 25°C$, $T_{left} = 200°C$, and $H = 1$. The temperature profile is affected by the value of the dimensionless parameter H as shown by Eq. (68). The larger H the larger the heat transfer to the ambient and the steeper the profile of the temperature at the beginning of the fin. The truncation errors for both methods are also affected by the value of H. In the case of the FDM, the truncation errors at the central nodes and at the right boundary are affected indirectly by H through the derivatives of the variable (see Eqs. (64) and (65)). In the case of the CVF method, the truncation errors are affected indirectly by H through the derivatives of the variable at the central nodes and right boundary node (see Eqs. (64) and (67)), and they are also directly affected by H at the right boundary node (see Eq. (67)). Numerical solutions were calculated for nj = 6. Important results are given next (ten significant figures were used for the calculations; however, the results are summarized here with two significant figures):

$$\mathbf{T} = \begin{pmatrix} 200.00 \\ 176.68 \\ 159.44 \\ 147.60 \\ 140.69 \\ 138.41 \end{pmatrix} \quad \mathbf{T}_{FDM} = \begin{pmatrix} 200.00 \\ 176.71 \\ 159.48 \\ 147.63 \\ 140.69 \\ 138.38 \end{pmatrix}$$

$$\mathbf{T}_{CVF} = \begin{pmatrix} 200.00 \\ 176.74 \\ 159.54 \\ 147.73 \\ 140.82 \\ 138.55 \end{pmatrix} \quad \mathbf{TE}_{FDM} = \begin{pmatrix} 0.0000 \\ -0.5063 \\ -0.4487 \\ -0.4092 \\ -0.3861 \\ -0.2283 \end{pmatrix}$$

$$\mathbf{TE}_{CVF} = \begin{pmatrix} 0.0000 \\ -0.5063 \\ -0.4487 \\ -0.4092 \\ -0.3861 \\ -0.3785 \end{pmatrix} \quad (\mathbf{T.E.})_{FDM} = \begin{pmatrix} 0.0000 \\ -0.5063 \\ -0.4487 \\ -0.4092 \\ -0.3861 \\ -0.2283 \end{pmatrix}$$

$$(\mathbf{T.E.})_{CVF} = \begin{pmatrix} 0.0000 \\ -0.5063 \\ -0.4487 \\ -0.4092 \\ -0.3861 \\ -0.3780 \end{pmatrix}$$

where $\mathbf{T}$ represents the analytical solution vector, $\mathbf{T}_{FDM}$, and $\mathbf{T}_{CVF}$ represent the numerical solution vectors using the FDM and the CVF, respectively. $\mathbf{TE}_{FDM}$ and $\mathbf{TE}_{CVF}$ represent the total truncation error vectors for the two different methods calculated using Eq. A15, $(\mathbf{T.E.})_{FDM}$ is the truncation error vector for the FDM predicted using Eqs. (64) and (65), and, and $(\mathbf{T.E.})_{CVF}$ is the truncation error vector for the CVF predicted using Eqs. (64) and (67).

The results shown above indicate that the truncation errors predicted for the CVF and FDM agree very well with the exact one calculated using Eq. A15. The deviation between the truncation error predicted for the CVF at the last node and the exact one is due to the approximations made during the derivation of Eq. (67). Using a larger number of nodes would reduce this deviation. The results shown above demonstrate the utility of the methodology used here to estimate the truncation errors for both methods including the effect of the boundary conditions. Additionally, the results demonstrate that the truncation error at the right boundary using FDM is order $(\Delta X)^2$ whereas for the CVF method is order (ΔX). The analysis of the boundary conditions has shown that the order of accuracy for the CVF-PLP method is reduced by one at the boundary respect to the central nodes. That is the truncation error at the right boundary for the CVF-PLP is order (ΔX) whereas is order $(\Delta X)^2$ for the central nodes. The same can be concluded for the CVF-SP method, therefore when using this method the truncation error at the boundary for a Robin type boundary condition will be order $(\Delta X)^0$.

4. Examples

4.1. Example 1: unsteady-state convective diffusion equation

The purpose of this example is to evaluate the conservation of mass in the system using the FDM, and CVF.

Consider a closed isothermal system (tank) containing two components, A and B. Component B is a gas and is insoluble in liquid A. Liquid A is allowed to evaporate slowly into gas B so the liquid level remains constant; after some time the system reaches equilibrium with the concentration of A in the gas phase at 45 gmol/m^3. Suddenly the top of the tank is removed giving rise to a uniform exit flow of 'A' that is equal to the evaporating flux of 'A'. Accordingly, the average concentrations of components 'A and 'B' over the volume remain constant with time. The equations that describe this situation, assuming flow only in the 'X' direction are:

$$\frac{\partial C_a}{\partial t} = \frac{D_{ab}}{L^2}\frac{\partial^2 C_a}{\partial X^2} - \frac{\nu}{L}\frac{\partial C_a}{\partial X} \tag{69}$$

$$C_a = C_{a0} \quad \text{at } t = 0 \ \forall \ X \tag{70}$$

$$N_a = \frac{-D_{ab}}{L}\frac{\partial C_a}{\partial X} + \nu C_a \quad \text{at } X = 0 \ \forall \ t > 0 \tag{71}$$

$$N_a = \frac{-D_{ab}}{L}\frac{\partial C_a}{\partial X} + \nu C_a \quad \text{at } X = 1 \ \forall \ t > 0 \tag{72}$$

where $X = x/L$. There is no closed-form analytical solution for this problem; nevertheless, because of the conservation of mass, the overall concentration of 'A' should be constant, and this constraint can be used to compare the two methods. The average concentration is given by the equation:

$$C_{a,avg} = \int_0^1 C_a(X)dX \tag{73}$$

where $C_{a,avg} = C_{a0}$ due to conservation of mass.

In the FDM, Eqs. (69)–(72) were discretised according to Fig. 1. In the CVF, the equations were discretised according to the profiles shown in Fig. 2, with SP used for the variable and PLP used for the variable or the derivative. Fig. 3 shows the application of the CVF at the boundaries. According to the discretisation procedure, the left boundary is located at position B_l(j = 1 in the discretisation) and the right boundary at position B_r(j = nj in the discretisation, see Fig. 3). Since the boundaries are the limits (spatial in this case), the mass balance has to be performed in half of the control volume, yielding with an internal interface between the boundary B_l and the internal left node I_l called iil (see Fig. 3); in the same way the internal interface of the boundary of the right (B_r) is called iir (see Fig. 3). According to the CVF, the integral mass balance in the left boundary over half of the control volume yields.

$$\int_{B_l}^{ii_l}\int_t^{t+\Delta t}\frac{\partial C_a}{\partial t}\,dt\,dX = -\frac{1}{L}\int_{B_l}^{ii_l}\int_t^{t+\Delta t}\frac{\partial N_a}{\partial X}\,dt\,dX \tag{74}$$

Solving the internal integral of the l.h.s. of Eq. (74), and assuming that the value of C_a at B_l prevails throughout the half control volume:

$$\int_{B_l}^{ii_l}\int_t^{t+\Delta t}\frac{\partial C_a}{\partial t}\,dt\,dX = (C_a|_{t+\Delta t,B_l} - C_a|_{t,B_l})\frac{\Delta X}{2} \tag{75}$$

For the r.h.s of Eq. (74), assuming that the value of $\partial N_a/\partial X$ at $t + \Delta t$ prevails throughout the time interval, and solving.

$$-\frac{1}{L}\int_{B_l}^{ii_l}\int_t^{t+\Delta t}\frac{\partial N_a}{\partial X}\,dt\,dX = -\frac{\Delta t}{L}(N_a|_{t+\Delta t,ii_l} - N_a|_{t+\Delta t,B_l}) \tag{76}$$

Substituting Eqs. (75) and (76) into Eq. (74) and rearranging.

$$\frac{(C_{a|t+\Delta t,B_l} - C_{a|t,B_l})}{\Delta t} = -\frac{2}{L\Delta X}(N_a|_{t+\Delta t,ii_l} - N_a|_{t+\Delta t,B_l}) \tag{77}$$

The flux of species 'A' at any position can be evaluated using the equation.

$$N_a = \frac{-D_{ab}}{L}\frac{\partial C_a}{\partial X} + \nu C_a \tag{78}$$

Evaluating Eq. (78) at the internal interface and substituting it into Eq. (77).

$$\frac{(C_{a|t+\Delta t,B_l} - C_{a|t,B_l})}{\Delta t} = -\frac{2}{L\Delta X}\left(-\frac{D_{ab}}{L}\frac{\partial C_a}{\partial X}|_{t+\Delta t,ii_l} + \nu C_a|_{t+\Delta t,ii_l} - N_a|_{t+\Delta t,B_l}\right) \tag{79}$$

Using the same procedure the equation for the right boundary can be obtained. The derivative terms in Eq. (79) can be approximated using PLP and the concentration terms can be approximated using not only PLP but also with SP. The discretised equations for both methods are compared in Table 4. The equations were solved using Newman's BAND(J) subroutine. The parameters used are given in Table 5.

Note that in Table 4 equation E.1.2a is the same that equation E.1.2b (both accurate to order $\Delta X^2 + \Delta t$); thus, the discretised governing equation is the same for the FDM and the CVF-PLP method. However, the equations given for the boundary conditions are different, this is because the boundary conditions in the CVF are obtained with a mass balance whereas those for the FDM are obtained by discretising Eqs. (71) and (72). An analysis of the accuracy of the methods can be performed as explained in the previous section. There was not significant difference in the computational time required by the two methods.

Fig. 4 presents the numerical solution for example 1. Fig. 4a shows the variation of the concentration through the tank at t = 20 s (with nj = 6 and $\Delta t = 2$ s) using the two methods. The profiles given by all of them have the same behavior, i.e. the concentration

Table 4
Comparison of the discretised equations, presented in functional form for programming (White, 1987), used for the FDM and CVF in example 1[a]

Method	Region	Discretised equation	Equations
FDM	$j=1$	$F(1)=N_a\|_{X=0}-\nu\phi_{1,j}+\frac{D_{ab}}{L}\left(\frac{-3\phi_{1,j}+4\phi_{1,j+1}-\phi_{1,j+2}}{2\Delta X}\right)$	E1.1a
	$1<j<nj$	$F(1)=\frac{D_{ab}}{L^2}\left(\frac{\phi_{1,j+1}-2\phi_{1,j}+\phi_{1,j-1}}{\Delta X^2}\right)-\frac{\nu}{L}\left(\frac{\phi_{1,j+1}-\phi_{1,j-1}}{2\Delta X}\right)-\frac{\phi_{1,j}}{\Delta t}+\frac{\phi N_{1,j}}{\Delta t}$	E1.2a
	$j=nj$	$F(1)=N_a\|_{X=1}-\nu\phi_{1,j}+\frac{D_{ab}}{L}\left(\frac{3\phi_{1,j}-4\phi_{1,j-1}+\phi_{1,j-2}}{2\Delta X}\right)$	E1.3a
CVF-PLP	$j=1$	$F(1)=\frac{2}{L\Delta X}\left\{N_a\|_{X=0}+\frac{D_{ab}}{L}\left(\frac{\phi_{1,j+1}-\phi_{1,j}}{\Delta X}\right)-\nu\left(\frac{\phi_{1,j+1}+\phi_{1,j}}{2}\right)\right\}-\frac{\phi_{1,j}}{\Delta t}+\frac{\phi N_{1,j}}{\Delta t}$	E1.1b
	$1<j<nj$	$F(1)=\frac{D_{ab}}{L^2}\left(\frac{\phi_{1,j+1}-2\phi_{1,j}+\phi_{1,j-1}}{\Delta X^2}\right)-\frac{\nu}{L}\left(\frac{\phi_{1,j+1}-\phi_{1,j-1}}{2\Delta X}\right)-\frac{\phi_{1,j}}{\Delta t}+\frac{\phi N_{1,j}}{\Delta t}$	E1.2b
	$j=nj$	$F(1)=-\frac{2}{L\Delta X}\left\{N_a\|_{X=1}+\frac{D_{ab}}{L}\left(\frac{\phi_{1,j}-\phi_{1,j-1}}{\Delta X}\right)-\nu\left(\frac{\phi_{1,j}+\phi_{1,j-1}}{2}\right)\right\}-\frac{\phi_{1,j}}{\Delta t}+\frac{\phi N_{1,j}}{\Delta t}$	E1.3b
CVF-SP	$j=1$	$F(1)=\frac{2}{L\Delta X}\left\{N_a\|_{X=0}+\frac{D_{ab}}{L}\left(\frac{\phi_{1,j+1}-\phi_{1,j}}{\Delta X}\right)-\nu\phi_{1,j}\right\}-\frac{\phi_{1,j}}{\Delta t}+\frac{\phi N_{1,j}}{\Delta t}$	E1.1c
	$1<j<nj$	$F(1)=\frac{D_{ab}}{L^2}\left(\frac{\phi_{1,j+1}-2\phi_{1,j}+\phi_{1,j-1}}{\Delta X^2}\right)+\frac{\nu}{L}\left(\frac{\phi_{1,j-1}-\phi_{1,j}}{\Delta X}\right)-\frac{\phi_{1,j}}{\Delta t}+\frac{\phi N_{1,j}}{\Delta t}$	E1.2c
	$j=nj$	$F(1)=\frac{2}{L\Delta X}\left\{-N_a\|_{X=1}-\frac{D_{ab}}{L}\left(\frac{\phi_{1,j}-\phi_{1,j-1}}{\Delta X}\right)+\nu\phi_{1,j-1}\right\}-\frac{v_{1,j}}{\Delta t}+\frac{\phi N_{1,j}}{\Delta t}$	E1.3c

[a] The equations used for the CVF were adapted to use the BAND(J) subroutine (Newman, 1973a). Where $F(1)=0$ and $\phi N_{1,j}$ represents the value of the variable at the previous time $(t-\Delta t)$.

decreases with the distance. The change of the concentration with the distance is due to the gradient of concentration caused by the fluxes at the entrance and exit of the tank. Fig. 4b shows the overall mass balance in the tank using the two methods at different times with $\Delta t=2$ s. The average concentration was obtained by solving numerically Eq. (73) using the trapezoid rule for integration; and due to conservation of mass it should stay constant at 45.0 gmol/m^3. However, for the FDM the average concentration decreases with time for $nj=6$ and 21; and it becomes mass conservative only when $nj=41$ or larger. The FDM also exhibited this behavior for smaller values of Δt (the mass balance was not significantly affected by Δt). In contrast, the CVF (for both SP and PLP) is mass conservative independently of the number of spatial nodes (nj) or the time step (Δt). This fact is due to the difference in how the methods deal with the boundary conditions. In the CVF the boundary conditions are incorporated into the governing equation while in the FDM they are not. This example demonstrates that mass conservation can be achieved with fewer node points when using the CVF than when using the FDM, when both boundary conditions are given as a flux (Robin type at both boundaries). The same conclusion follows for Neumann type boundary conditions.

4.2. Example 2: steady-state heat conduction with a forcing function

The purpose of this example is to evaluate the accuracy of the FDM and CVF when an additional flux boundary condition is used in the system due to its heterogeneity. Heat conduction in a nuclear fuel rod assembly is represented in dimensionless variables by the following equation and boundary conditions (Bird, Stewart & Lightfoot, 1960):

$$\frac{\partial}{\partial\Re}\left(\Re K_f\frac{\partial T}{\partial\Re}\right)+S_o\Re R_c^2\left[1+b\left(\frac{R_c\Re}{R_f}\right)^2\right]=0 \quad \text{at } 0<\Re<0.75 \tag{80}$$

$$\frac{\partial}{\partial\Re}\left(\Re K_c\frac{\partial T}{\partial\Re}\right)=0 \quad \text{at } 0.75<\Re<1.0 \tag{81}$$

Table 5
Parameters used in examples 1 and 2

Example	Parameter	Value	Units
1	C_{a0}	45.0	Gmol/m^3
	D_{ab}	1×10^{-5}	m^2/s
	L	1×10^{-1}	M
	ν	1×10^{-6}	m/s
	N_a (at $X=0$ & $X=1$)	9×10^{-3}	Gmol/m^2 s
2	K_c	0.640	Cal/s °C cm
	K_f	0.066	Cal/s °C cm
	R_f	0.9525	Cm
	R_c	1.27	Cm
	T_l	500	°C
	b	0.1	Dimensionless
	S_o	50	Cal/s cm^3

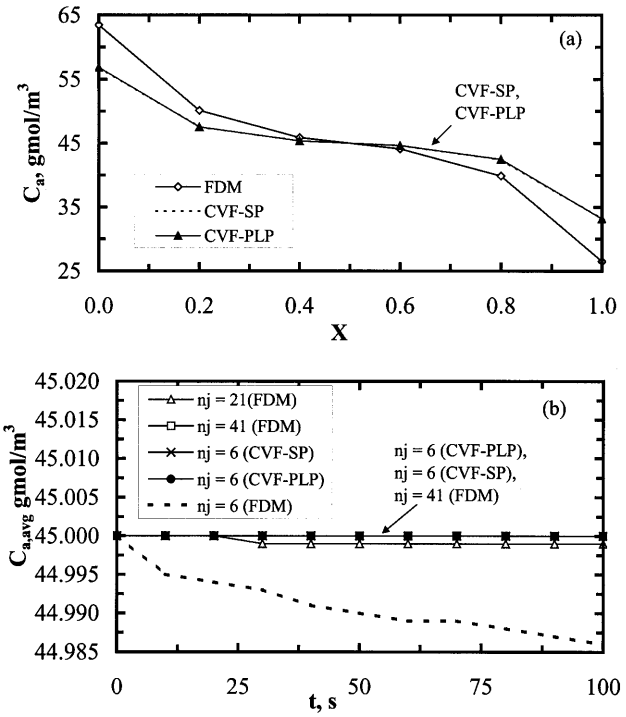

Fig. 4. Numerical solutions for example 1 from the FDM and CVF (a) variation of the concentration through the tank at $t = 20$ s ($nj = 6$); (b) overall mass balance in the tank ($\Delta t = 2$ s).

$$\frac{\partial T}{\partial \Re} = 0 \quad \text{at } \Re = 0 \tag{82}$$

$$K_f \frac{\partial T}{\partial \Re} = K_c \frac{\partial T}{\partial \Re} \quad \text{at } \Re = 0.75 \tag{83}$$

$$T = T_1 \text{ at } \Re = 1 \tag{84}$$

where $\Re = r/R_c$. Eq. (84) assumes an infinite heat transfer coefficient.

For this problem, the analytical solution is given by (Bird et al., 1960):

$$T = T_1 - \frac{S_o \Re^2 R_c^2}{4K_f}\left[1 + \frac{b}{4}\left(\frac{\Re R_c}{R_f}\right)^2\right] + \frac{S_o R_f^2}{2K_c}\left[1 + \frac{b}{2}\right] \ln\left(\frac{R_c}{R_f}\right) + \frac{S_o R_f^2}{4K_f}\left[1 + \frac{b}{4}\right] \quad \text{at } 0 \le \Re \le \frac{R_f}{R_c} \tag{85}$$

$$T = T_1 + \frac{S_o R_f^2}{2K_c}\left[1 + \frac{b}{2}\right]\ln\left(\frac{1}{\Re}\right) \quad \text{at } \frac{R_f}{R_c} \le \Re \le 1 \tag{86}$$

The parameters used for solving the problem are shown in Table 5. The discretised equations for the FDM were obtained in the same way as before, except for the interface. At the interface ($\Re = 0.75$), the discretised equation was obtained by applying three-point forward and three-point backward to the l.h.s. and r.h.s. of Eq. (83). In the CVF the discretised equations for the region $0 < \Re < 0.75$ are obtained by integrating Eq. (80) from east to west as shown

$$\int_w^e \frac{\partial}{\partial \Re}\left(\Re K_f \frac{\partial T}{\partial \Re}\right) d\Re + \int_w^e S_o \Re R_c^2 \left[1 + b\left(\frac{R_c \Re}{R_f}\right)^2\right] d\Re = 0 \tag{87}$$

$$\frac{K_f}{\Delta \Re}\left(\Re_e \left.\frac{dT}{d\Re}\right|_e - \Re_w \left.\frac{dT}{d\Re}\right|_w\right) + S_o \Re_j R_c^2 \left[1 + b\left(\frac{R_c \Re_j}{R_f}\right)^2\right] = 0 \tag{88}$$

where $\Re_e = \Re_j + \Delta\Re/2$ and $\Re_w = \Re_j - \Delta\Re/2$. The discretised equations when $0.75 < \Re < 1.0$ are obtained in the same way but integrating Eq. (81). At the interface Eq. (80) is integrated from 'e' to 'j' (half of the control volume) and Eq. (81) is integrated from 'j' to 'w', the discretised equation at this node is obtained by adding both results. The discretised equations for this example are given in Table 6. In all the cases, the discretised equations were solved using Maple V. There was not significant difference in the computational time required by the two methods.

Using the methodology explained before the truncation errors for the approximation at the central nodes can be obtained and they are summarized by.

$$(T.E.)_{FDM} = (T.E.)_{CVF} = -\Delta\Re(j-1)\frac{\Delta\Re^2}{12}\phi_j^{IV} - \frac{\Delta\Re^2}{6}\phi_j''' - \ldots \tag{89}$$

Eq. (89) has been simplified. The more significant terms for the calculation of the truncation errors have been included. The truncation errors for both methods at the central nodes are the same. The truncation errors at the left boundary and at the interface will be different for both methods. Using the methodology explained in Section 1 the truncation errors for the CVF at the boundaries can be obtained. For instance, the truncation errors at the left boundaries are given by.

$$(T.E)_{FDM} = \frac{\Delta\Re^2}{3}\phi_1''' + \frac{\Delta\Re^3}{4}\phi_1^{IV} \tag{90}$$

$$(T.E)_{CVF} = -\frac{\Delta\Re}{2}\phi_1'' - \frac{\Delta\Re^2}{6}\phi_1''' - \frac{\Delta\Re^3}{24}\phi_1^{IV} \tag{91}$$

The truncation error at the left boundary for the CVF method is ($\Delta\Re$)order of accuracy whereas for the FDM is order $(\Delta\Re)^2$. It can be shown that at the interface, the truncation error for the CVF method is only ($\Delta\Re$) order of accuracy whereas for the FDM is order $(\Delta\Re)^2$. From this analysis we can conclude that the truncation errors for the left and interface boundaries using the CVF are larger than when using the FDM. Therefore, the FDM will be more accurate than the CVF.

Fig. 5 presents the comparison of the errors (analytical — numerical solution) for both methods. The FDM is more accurate than the CVF for a small and large number of nodes ($nj = 21$ and 101). The CVF is less accurate than the FDM, because of the effect of the

Table 6
Comparison of the discretised equations, presented in functional form for programming (White, 1987), used for the FDM and CVF in example 2[a]

Method	Region	Discretised equation	Equations
FDM	$j = 1$	$F(1) = \left(\frac{-3\phi_{1,j} + 4\phi_{1,j+1} - \phi_{1,j+2}}{2\Delta\Re}\right)$	E2.1a
	$1 < j < nj(2)$	$F(1) = (j-1)\Delta\Re\left(\frac{\phi_{1,j+1} - 2\phi_{1,j} + \phi_{1,j-1}}{\Delta\Re^2}\right) + \left(\frac{\phi_{1,j+1} - \phi_{1,j-1}}{2\Delta\Re}\right) + \frac{S_o R_c^2 (j-1)\Delta\Re}{K_f}\left[1 + b\left(\frac{R_c\Delta\Re}{R_f}\right)^2 (j-1)^2\right]$	E2.2a
	$j = nj(2)$	$F(1) = K_f\left(\frac{3\phi_{1,j} - 4\phi_{1,j-1} + \phi_{1,j-2}}{2\Delta\Re}\right) - K_c\left(\frac{-3\phi_{1,j} + 4\phi_{1,j+1} - \phi_{1,j+2}}{2\Delta\Re}\right)$	E2.3a
	$nj(2) < j < nj$	$F(1) = (j-1)\Delta\Re\left(\frac{\phi_{1,j+1} - 2\phi_{1,j} + \phi_{1,j-1}}{\Delta\Re^2}\right) + \left(\frac{\phi_{1,j+1} - \phi_{1,j-1}}{2\Delta\Re}\right)$	E2.4a
	$j = nj$	$F(1) = \phi_{1,j} - T_1$	E2.5a
CVF-PLP	$j = 1$	$F(1) = \left(\frac{\phi_{1,j+1} - \phi_{1,j}}{\Delta\Re}\right)$	E2.1b
	$1 < j < nj(2)$	$F(1) = (j-1)\Delta\Re\left(\frac{\phi_{1,j+1} - 2\phi_{1,j} + \phi_{1,j-1}}{\Delta\Re^2}\right) + \left(\frac{\phi_{1,j+1} - \phi_{1,j-1}}{2\Delta\Re}\right) + \frac{S_o R_c^2 (j-1)\Delta\Re}{K_f}\left[1 + b\left(\frac{R_c\Delta\Re}{R_f}\right)^2 (j-1)^2\right]$	E2.2b
	$j = nj(2)$	$F(1) = K_f\left(j - \frac{3}{2}\right)\left(\frac{\phi_{1,j} - \phi_{1,j-1}}{\Delta\Re}\right) - K_c\left(j - \frac{1}{2}\right)\left(\frac{\phi_{1,j+1} - \phi_{1,j}}{\Delta\Re}\right) - \frac{S_o R_c^2 (j-1)\Delta\Re}{2}\left[1 + b\left(\frac{R_c\Delta\Re}{R_f}\right)^2 (j-1)^2\right]$	E2.3b
	$nj(2) < j < nj$	$F(1) = (j-1)\Delta\Re\left(\frac{\phi_{1,j+1} - 2\phi_{1,j} + \phi_{1,j-1}}{\Delta\Re^2}\right) + \left(\frac{\phi_{1,j+1} - \phi_{1,j-1}}{2\Delta\Re}\right)$	E2.4b
	$j = nj$	$F(1) = \phi_{1,j} - T_1$	E2.5b

[a] The equations were solved using Maple V. Where $F(1) = 0$.

approximations used for the left boundary and the interface.

5. Conclusions

A comparison between the FDM, and the CVF was made including the use of two different profiles (SP and PLP). The conservativeness, accuracy, advantages and disadvantages of the methods were evaluated.

The FDM is not mass conservative when a small number of nodes is used in a system represented by a second order differential equation when both boundary conditions are Robin type or Neumann type. The lack of conservation is caused because the boundary conditions are not included into the governing equation. Using the FDM with a large number of nodes can solve this problem. In contrast, the CVF is mass conservative for any number of nodes. Therefore, when dealing with Robin or Neumann type of boundary conditions at each boundary, the CVF is superior to the FDM when a small number of nodes is used.

There are no major differences in the computational time required by the two methods to solve the equations. Both methods are easy to implement. However, the CVF requires the formulation and integration of the energy and/or mass balances at any boundary or region in the system, while for the FDM the balances are formulated first and after a direct substitution of the derivatives by discretised variables is performed.

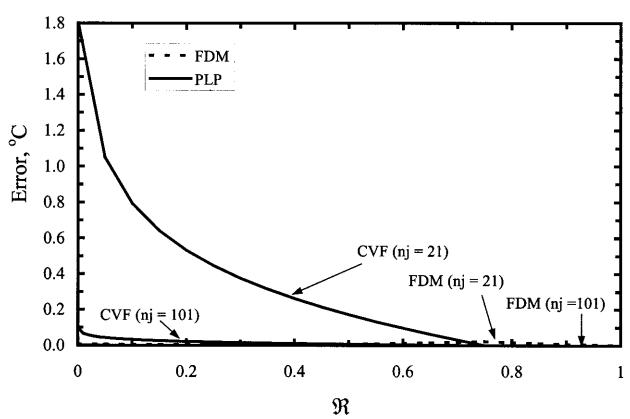

Fig. 5. Comparison of the errors (|analytical minus numerical solution|) at different node points given by the FDM and CVF for example 2.

The technique proposed by Leonard (1994, 1995) to determine the truncation errors for the CVF was evaluated. The truncation errors calculated with his technique mislead the interpretation of the results. The technique is only valid for the approximation of the variables and derivatives at the faces of the control volume as a function of the node points. However, the truncation errors associated with the average of the variables over the control volume are not considered by his method. The truncation error for the CVF should be determined using the mean-value theorem for integral calculus that incorporates the truncation error associated with the average of the variables over the control volume. The total truncation error for the approximation will be the one obtained by adding the truncation error associated with expressing the variables and/or the derivatives as a function of the node points, and the truncation error cause by solving the algebraic equations at the node points and not at the volume faces. The use of this method allows obtaining truncation errors for the CVF that agree with the numerical results obtained.

We have shown that the boundary conditions should be incorporated in the truncation error analysis of a problem to evaluate the accuracy of the method. A procedure to evaluate the accuracy of the methods based on the truncation error of the approximations has been developed. Its applicability has been tested for some systems. The accuracy of the methods for the same number of nodes depends on the behavior of the variable, type of boundary conditions, and profiles used for the discretisation of the equations. The analysis of truncation errors proposed here can be used for predicting the accuracy of the method before solving a particular problem. The following rules-of-thumb for accuracy of the methods were derived from the truncation error analysis. (1) The truncation error for Neumann and/or Robin type boundary conditions is order $(\Delta X)^2$ for the FDM whereas is order (ΔX) for the CVF-PLP method. (2) The FDM is more accurate than the CVF-PLP for problems with interfaces between adjacent regions. (3) The FDM is more accurate than the CVF for systems where a combination of Dirichlet and Neumann, or Dirichlet and Robin type boundary conditions are used unless the response of the dependent variable is very steep. (4) CVF usually requires more number of nodes than the FDM to obtain the same accuracy. (5) The methods are essentially the same when in a one-dimensional system, the boundary conditions are given directly as a value of the variable, the system consists of linear differential equations, and the coordinate system is Cartesian.

6. Nomenclature

A	jacobians coefficient matrix
$\bar{A}_j$	jacobian defined by Eq. A16
B	constants vector
$\bar{B}_j$	jacobian defined by Eq. A16
b	constant used in example 2, 0.1 dimensionless
b_l	parameter used in Eq. (39), 1 dimensionless
B_l	left boundary in CVF
B_r	right boundary in CVF
BW	backward approximation
C	concentration, gmol/m^3
C_a	concentration of component A, gmol/m^3
C_{a0}	initial concentration of A, 45 gmol/m^3 (see Table 5)
$C_{a,avg}$	average concentration, gmol/m^3
CVF	control volume formulation
$\bar{D}_j$	jacobian defined by Eq. A.16
D_{ab}	diffusivity of specie A on B, 1×10^{-5} m^2/s (see Table 5)
e	east face of the control volume
E	discretised point in the east direction of the CVF
Error	error vector (contains the values for Analytical-Numerical Solution)
F	equations vector
FDM	finite difference method
H	parameter used in Eq. (56), 1 dimensionless
ii_l	interface for the left boundary in CVF
ii_r	interface for the right boundary in CVF
I_l	internal left node in CVF
I_r	internal right node in CVF
j	spatial direction nodal
K_c	thermal conductivity of the cladding, 0.64 cal/°C cm s (see Table 5)
K_f	thermal conductivity of the nuclear fuel rod, 0.066 cal/°C cm s (see Table 5)
L	length, m
n_j	number of spatial nodes
N_a	flux of species A, 9×10^{-3} gmol/m^2 s (see Table 5)
P	discretised point under study in the CVF
3PB	three-point backward approximation
3PF	three-point forward approximation
PLP	piece-wise linear profile
r	radial coordinate, cm
$\Re$	radial coordinate ($\Re = r/R_c$), dimensionless
R_c	radius of the cladding, 1.27 cm (see Table 5)
R_f	radius of the nuclear fuel rod, 0.9525 cm (see Table 5)

S_o	constant fission heat, 50 cal/cm^3 s (see Table 5)
SP	step wise profile
t	time, s
T	temperature, °C
T	analytical solution vector for the temperature, °C
$\bar{T}$	control volume average temperature, °C
T_a	ambient temperature used in Eq. (56), °C
$\mathbf{T}_{\text{FDM-CVF}}$	numerical solution vector for the temperature, °C
T_1	outside temperature, 500°C
T_{left}	temperature at left boundary, °C
T_{right}	temperature at right boundary, °C
T_o	initial temperature, 100°C
TE	truncation error vector calculated from the numerical solution according to the Appendix A
$(\mathbf{T.E.})_{\text{CVF-PLP}}$	truncation error vector for the CVF-PLP
$(T.E.)_{\text{CVF-PLP}}$	truncation error of the equation using CVF-PLP
$(T.E.)_{\text{CVF-SP}}$	truncation error of the equation using CVF-SP
$(T.E.)_{\text{Cyl–e,w}\rightarrow\text{j}}$	truncation error associated with the derivatives evaluated at the faces of the control volume in cylindrical coordinates.
$(T.E.)_{\text{D,B}_l+\text{ii}_l\rightarrow\text{j}}$	truncation error associated with the derivative evaluated at the left boundary interfaces.
$(T.E.)_{\text{D,B}_r+\text{ii}_r\rightarrow\text{j}}$	truncation error associated with the derivative evaluated at the right boundary interfaces.
$(T.E.)_{\text{D}-\text{e,w}\rightarrow\text{j}}$	truncation error associated with the derivatives evaluated at the faces of the control volume.
$(T.E.)_{\text{D,e}+\text{w}\rightarrow\text{j}}$	truncation error associated with the derivatives at the east plus west faces of the control volume
$(T.E.)_{\text{D}-1\rightarrow\text{j}}$	truncation error associated with solving the derivatives at the left boudary
$(T.E.)_{\text{D}-\text{r}\rightarrow\text{j}}$	truncation error associated with solving the derivatives at the right boudary
$(T.E.)_{\text{e}-\text{PLP},1\rightarrow\text{j}}$	truncation error for the derivative evaluated at the east face using PLP
$(T.E.)_{\text{e}-\text{PLP,V}}$	truncation error for the variable evaluated at the east face using PLP
$(T.E.)_{\text{e}-\text{SP}}$	truncation error of the variable evaluated at the east face using SP
$(T.E.)_{\text{e}-\text{w,PLP}-1}$	truncation error for the derivative evaluated at the east minus west faces using PLP
$(T.E.)_{\text{e}-\text{w,PLP}-\text{V}}$	truncation error for the variable evaluated at the east minus west faces using PLP
$(T.E.)_{\text{e}-\text{w,SP}}$	truncation error for the variable evaluated at the east minus west faces using SP
$(\mathbf{T.E.})_{\text{FDM}}$	truncation error vector for the FDM
$(T.E.)_{\text{FDM}}$	truncation error of the equation using FDM
$(T.E.)_{1-\text{FDM}}$	truncation error of the first derivative using FDM
$(T.E.)_{1\text{BW}-\text{FDM}}$	truncation error of the first derivative using FDM with backward approximation
$(T.E.)_{2-\text{FDM}}$	truncation error of the second derivative using FDM
$(T.E.)_{3\text{PB}-\text{FDM}}$	truncation error using 3PB approximation
$(T.E.)_{3\text{PF}-\text{FDM}}$	truncation error using 3PF approximation
$(T.E.)_{\text{V,B}_l+\text{ii}_l\rightarrow\text{j}}$	truncation error associated with the variable evaluated at the left boundary interfaces.
$(T.E.)_{\text{V,B}_r+\text{ii}_r\rightarrow\text{j}}$	truncation error associated with the variable evaluated at the right boundary interfaces.
$(T.E.)_{\text{V(j)}-\text{D(j)}}$	truncation error associated with expressing the variables and/or derivatives as a function of the node points
$(T.E.)_{\text{V,D}\rightarrow\text{j}}$	truncation error caused by solving the algebraic equations at the node points
$(T.E.)_{\text{V}-\text{e,w}\rightarrow\text{j}}$	truncation error associated with the variables evaluated at the faces of the control volume.
$(T.E.)_{\text{V,e}+\text{w}\rightarrow\text{j}}$	truncation error associated with the variables at the east plus west faces of the control volume
$(T.E.)_{\text{V}-1\rightarrow\text{j}}$	truncation error associated with the variables evaluated at left boundary of the control volume
$(T.E.)_{\bar{V}-1\rightarrow\text{j}}$	truncation error associated with the average of the variables evaluated at left boundary of the control volume.
$(T.E.)_{\text{V}-\text{r}\rightarrow\text{j}}$	truncation error associated with the variables evaluated at right boundary of the control volume
$(T.E.)_{\bar{V}-\text{r}\rightarrow\text{j}}$	truncation error associated with the average of the variables evaluated at right boundary of the control volume.
$(T.E.)_{\text{w}-\text{PLP},1}$	truncation error for the derivative evaluated at the west face using PLP
$(T.E.)_{\text{w}-\text{PLP,V}}$	truncation error for the variable evaluated at the west face using PLP

$(T.E.)_{w-SP}$	truncation error for the variable evaluated at the west face using SP
v	velocity, 1×10^{-6} m/s (see Table 5)
w	west face of the control volume
W	discretised point in the west direction of CVF
x	distance in x spatial direction, m
X	dimensionless distance
$\bar{X}_j$	jacobian defined by Eq. A.16
$\bar{Y}_j$	jacobian defined by Eq. A.16

Greek letters

ξ	value for the dependent variable that satisfies the mean-value theorem for integral calculus, see Eq. (33)
$\Delta\Re$	radial step size, dimensionless
Δt	step size in time, s
ΔX	step size in the X-direction, dimensionless
$(\Delta X)_e$	step size in the east direction, dimensionless
$(\Delta X)_w$	step size in the west direction, dimensionless
ϕ	dependent variable, dimensionless
ϕN	representation of the discretised dependent variable on time evaluated at time $t-\Delta t$
ϕ_E	variable evaluated at the point E
ϕ_P	variable evaluated at the point P
ϕ_W	variable evaluated at the point W

Appendix A. Calculation of the truncation error using the numerical solution

In the following analysis, it is assumed that the problem is linear, one-dimensional, and steady state. Let us start by showing the methodology to solve Eqs. (39)–(41) using FDM and CVF. The first step in the FDM is to discretise the equations. In the same way the first step for the CVF is to integrate the equations and after substitute the derivatives at the face volumes by discrete values using a specific approach. A uniform grid of mesh size ΔX is used. As stated in the paper, for this case the algebraic equations to solve simultaneously using the two different methods (FDM and CVF) are the same. Using 6 nodes for the solution (nj = 6) the algebraic equations to solve are given by.

$$\begin{aligned}
&F_1=\phi_1-T_{left}=0\\
&F_2=25\phi_1-51\phi_2+25\phi_3=0\\
&F_3=25\phi_2-51\phi_3+25\phi_4=0\\
&F_4=25\phi_3-51\phi_4+25\phi_5=0\\
&F_5=25\phi_4-51\phi_5+25\phi_6=0\\
&F_6=\phi_6-T_{right}=0
\end{aligned}\tag{A.1}$$

The set of equations given before can be represented in matrix–vector form by:

$$F=AT_{FDM\text{-}CVF}-B=0\tag{A.2}$$

where **F** represents the vector of the equations, $\mathbf{T}_{FDM-CVF}$ is the vector form with the dependent variables (ϕ_j), **A** is the coefficient matrix, and **B** is the constants vector (boundary conditions in this case). The vector $\mathbf{T}_{FDM\text{-}CVF}$, the matrix **A**, and the vector **B** are given by

$$\mathbf{T}_{FDM-CVF}=\begin{pmatrix}\phi_1\\ \phi_2\\ \phi_3\\ \phi_4\\ \phi_5\\ \phi_6\end{pmatrix}$$

$$A=\begin{pmatrix}
\frac{\partial F_1}{\partial\phi_1} & \frac{\partial F_1}{\partial\phi_2} & \frac{\partial F_1}{\partial\phi_3} & 0 & 0 & 0\\
\frac{\partial F_2}{\partial\phi_1} & \frac{\partial F_2}{\partial\phi_2} & \frac{\partial F_2}{\partial\phi_3} & 0 & 0 & 0\\
0 & \frac{\partial F_3}{\partial\phi_2} & \frac{\partial F_3}{\partial\phi_3} & \frac{\partial F_3}{\partial\phi_4} & 0 & 0\\
0 & 0 & \frac{\partial F_4}{\partial\phi_3} & \frac{\partial F_4}{\partial\phi_4} & \frac{\partial F_4}{\partial\phi_5} & 0\\
0 & 0 & 0 & \frac{\partial F_5}{\partial\phi_4} & \frac{\partial F_5}{\partial\phi_5} & \frac{\partial F_5}{\partial\phi_6}\\
0 & 0 & 0 & \frac{\partial F_6}{\partial\phi_4} & \frac{\partial F_6}{\partial\phi_5} & \frac{\partial F_6}{\partial v_6}
\end{pmatrix}\qquad B=\begin{pmatrix}T_{left}\\0\\0\\0\\0\\T_{right}\end{pmatrix}$$

The matrix **A** includes maximum three points different than zero because the approximations and the approaches used in this paper use maximum three points for the calculations. In this case, the matrix is given by.

$$A=\begin{pmatrix}1&0&0&0&0&0\\25&-51&25&0&0&0\\0&25&-51&25&0&0\\0&0&25&-51&25&0\\0&0&0&25&-51&25\\0&0&0&0&0&1\end{pmatrix}\tag{A.3}$$

The solution of Eq. (A.2) is given by.

$$T_{FDM\text{-}CVF}=A^{-1}B\tag{A.4}$$

Calling the elements of the inverse matrix λ, the inverse matrix for this case looks like.

$$A^{-1} = \begin{pmatrix} \lambda_{1,1} & \lambda_{1,2} & \lambda_{1,3} & \lambda_{1,4} & \lambda_{1,5} & \lambda_{1,6} \\ \lambda_{2,1} & \lambda_{2,2} & \lambda_{2,3} & \lambda_{2,4} & \lambda_{2,5} & \lambda_{2,6} \\ \lambda_{3,1} & \lambda_{3,2} & \lambda_{3,3} & \lambda_{3,4} & \lambda_{3,5} & \lambda_{3,6} \\ \lambda_{4,1} & \lambda_{4,2} & \lambda_{4,3} & \lambda_{4,4} & \lambda_{4,5} & \lambda_{4,6} \\ \lambda_{5,1} & \lambda_{5,2} & \lambda_{5,3} & \lambda_{5,4} & \lambda_{5,5} & \lambda_{5,6} \\ \lambda_{6,1} & \lambda_{6,2} & \lambda_{6,3} & \lambda_{6,4} & \lambda_{6,5} & \lambda_{6,6} \end{pmatrix} \quad (A.5)$$

For this case the values of the coefficients of the first and sixth rows are zero except for $\lambda_{1,1} = \lambda_{6,6} = 1$.

Substituting Eq. (A.5) into Eq. (A.4) and evaluating.

$$\mathbf{T_{FDM\text{-}CVF}} = \begin{pmatrix} \phi_1 \\ \phi_2 \\ \phi_3 \\ \phi_4 \\ \phi_5 \\ \phi_6 \end{pmatrix} = \begin{pmatrix} \lambda_{1,1}T_{left} + \lambda_{1,6}T_{right} \\ \lambda_{2,1}T_{left} + \lambda_{2,6}T_{right} \\ \lambda_{3,1}T_{left} + \lambda_{3,6}T_{right} \\ \lambda_{4,1}T_{left} + \lambda_{4,6}T_{right} \\ \lambda_{5,1}T_{left} + \lambda_{5,6}T_{right} \\ \lambda_{6,1}T_{left} + \lambda_{6,6}T_{right} \end{pmatrix} \quad (A.6)$$

Eq. (A.6) represents the numerical solution of the problem. Since the values of λ are known the solution can be calculated. The solution given by Eq. (A.6) does not represent exactly the analytical solution because of the terms that were neglected in the discretisation that represent the truncation error. Suppose that the vector **T** contains the values of the analytical solution evaluated at the specific node points, the error vector (**Error**) will be given by

$$\text{Error} = \mathrm{T} - T_{\mathrm{FDM-CVF}} \text{ or } \begin{pmatrix} \text{Error}_1 \\ \text{Error}_2 \\ \text{Error}_3 \\ \text{Error}_4 \\ \text{Error}_5 \\ \text{Error}_6 \end{pmatrix} = \begin{pmatrix} T_1 \\ T_2 \\ T_3 \\ T_4 \\ T_5 \\ T_6 \end{pmatrix} - \begin{pmatrix} \phi_1 \\ \phi_2 \\ \phi_3 \\ \phi_4 \\ \phi_5 \\ \phi_6 \end{pmatrix} \quad (A.7)$$

where the elements of the vectors **Error** and **T** have been called Error_j and T_j, respectively. If all the terms were included in the discretised equations the error would be zero.

Let us call **TE** the vector containing the terms not included in the discretised equations at each node point, that is, the vector containing the truncation errors at each node point that has the following elements

$$TE = \begin{pmatrix} TE_1 \\ TE_2 \\ TE_3 \\ TE_4 \\ TE_5 \\ TE_6 \end{pmatrix} \quad (A.8)$$

that is TE_1 represents the truncation error at node 1 and so on. To make the solution of Eq. (A.2) exact the truncation errors should be added, therefore.

$$\mathbf{F} = \mathbf{A}\mathbf{T}_{\mathrm{FDM-CVF}} - \mathbf{B} + \mathbf{TE} = 0 \quad (A.9)$$

The vectors **B** and **TE** can be combined together to redefine a new vector **B** given by.

$$B = \begin{pmatrix} \mathbf{T}_{left} - TE_1 \\ -TE_2 \\ -TE_3 \\ -TE_4 \\ -TE_5 \\ \mathbf{T}_{right} - TE_6 \end{pmatrix} \quad (A.10)$$

The coefficient matrix **A** is not affected by introducing the truncation errors, therefore the solution of the problem is given by.

$$T_{\mathrm{FDM-CVF}} = \begin{pmatrix} \lambda_{1,1} & \lambda_{1,2} & \lambda_{1,3} & \lambda_{1,4} & \lambda_{1,5} & \lambda_{1,6} \\ \lambda_{2,1} & \lambda_{2,2} & \lambda_{2,3} & \lambda_{2,4} & \lambda_{2,5} & \lambda_{2,6} \\ \lambda_{3,1} & \lambda_{3,2} & \lambda_{3,3} & \lambda_{3,4} & \lambda_{3,5} & \lambda_{3,6} \\ \lambda_{4,1} & \lambda_{4,2} & \lambda_{4,3} & \lambda_{4,4} & \lambda_{4,5} & \lambda_{4,6} \\ \lambda_{5,1} & \lambda_{5,2} & \lambda_{5,3} & \lambda_{5,4} & \lambda_{5,5} & \lambda_{5,6} \\ \lambda_{6,1} & \lambda_{6,2} & \lambda_{6,3} & \lambda_{6,4} & \lambda_{6,5} & \lambda_{6,6} \end{pmatrix} \begin{pmatrix} \mathbf{T}_{left} - TE_1 \\ -TE_2 \\ -TE_3 \\ -TE_4 \\ -TE_5 \\ \mathbf{T}_{right} - TE_6 \end{pmatrix} \quad (A.11)$$

Evaluating Eq. (A.11) yields.

$$T_{\mathrm{FDM-CVF}} = \begin{pmatrix} \phi_1 \\ \phi_2 \\ \phi_3 \\ \phi_4 \\ \phi_5 \\ \phi_6 \end{pmatrix} =$$

$$\begin{pmatrix} \lambda_{1,1}\mathbf{T}_{\text{left}} + \lambda_{1,6}\mathbf{T}_{\text{right}} - [\lambda_{1,1}\mathbf{TE}_1 + \lambda_{1,2}\mathbf{TE}_2 + \lambda_{1,3}\mathbf{TE}_3 + \lambda_{1,4}\mathbf{TE}_4 + \lambda_{1,5}\mathbf{TE}_5 + \lambda_{1,6}\mathbf{TE}_6] \\ \lambda_{2,1}\mathbf{T}_{\text{left}} + \lambda_{2,6}\mathbf{T}_{\text{right}} - [\lambda_{2,1}\mathbf{TE}_1 + \lambda_{2,2}\mathbf{TE}_2 + \lambda_{2,3}\mathbf{TE}_3 + \lambda_{2,4}\mathbf{TE}_4 + \lambda_{2,5}\mathbf{TE}_5 + \lambda_{2,6}\mathbf{TE}_6] \\ \lambda_{3,1}\mathbf{T}_{\text{left}} + \lambda_{3,6}\mathbf{T}_{\text{right}} - [\lambda_{3,1}\mathbf{TE}_1 + \lambda_{3,2}\mathbf{TE}_2 + \lambda_{3,3}\mathbf{TE}_3 + \lambda_{3,4}\mathbf{TE}_4 + \lambda_{3,5}\mathbf{TE}_5 + \lambda_{3,6}\mathbf{TE}_6] \\ \lambda_{4,1}\mathbf{T}_{\text{left}} + \lambda_{4,6}\mathbf{T}_{\text{right}} - [\lambda_{4,1}\mathbf{TE}_1 + \lambda_{4,2}\mathbf{TE}_2 + \lambda_{4,3}\mathbf{TE}_3 + \lambda_{4,4}\mathbf{TE}_4 + \lambda_{4,5}\mathbf{TE}_5 + \lambda_{4,6}\mathbf{TE}_6] \\ \lambda_{5,1}\mathbf{T}_{\text{left}} + \lambda_{5,6}\mathbf{T}_{\text{right}} - [\lambda_{5,1}\mathbf{TE}_1 + \lambda_{5,2}\mathbf{TE}_2 + \lambda_{5,3}\mathbf{TE}_3 + \lambda_{5,4}\mathbf{TE}_4 + \lambda_{5,5}\mathbf{TE}_5 + \lambda_{5,6}\mathbf{TE}_6] \\ \lambda_{6,1}\mathbf{T}_{\text{left}} + \lambda_{6,6}\mathbf{T}_{\text{right}} - [\lambda_{6,1}\mathbf{TE}_1 + \lambda_{6,2}\mathbf{TE}_2 + \lambda_{6,3}\mathbf{TE}_3 + \lambda_{6,4}\mathbf{TE}_4 + \lambda_{6,5}\mathbf{TE}_5 + \lambda_{6,6}\mathbf{TE}_6] \end{pmatrix} \tag{A.12}$$

The terms out of the bracket in Eq. (A.12) represent the numerical solution given in Eq. (A.6) which values are known, while the terms inside the bracket represent the error caused in the solution due to the truncation errors which values are unknown. Substituting Eq. (A.12) into Eq. (A.7) yields.

$$\begin{pmatrix} 0 \\ 0 \\ 0 \\ 0 \\ 0 \\ 0 \end{pmatrix} = \begin{pmatrix} \mathbf{T}_1 \\ \mathbf{T}_2 \\ \mathbf{T}_3 \\ \mathbf{T}_4 \\ \mathbf{T}_5 \\ \mathbf{T}_6 \end{pmatrix}$$

$$- \begin{pmatrix} \lambda_{1,1}\mathbf{T}_{\text{left}} + \lambda_{1,6}\mathbf{T}_{\text{right}} - [\lambda_{1,1}\mathbf{TE}_1 + \lambda_{1,2}\mathbf{TE}_2 + \lambda_{1,3}\mathbf{TE}_3 + \lambda_{1,4}\mathbf{TE}_4 + \lambda_{1,5}\mathbf{TE}_5 + \lambda_{1,6}\mathbf{TE}_6] \\ \lambda_{2,1}\mathbf{T}_{\text{left}} + \lambda_{2,6}\mathbf{T}_{\text{right}} - [\lambda_{2,1}\mathbf{TE}_1 + \lambda_{2,2}\mathbf{TE}_2 + \lambda_{2,3}\mathbf{TE}_3 + \lambda_{2,4}\mathbf{TE}_4 + \lambda_{2,5}\mathbf{TE}_5 + \lambda_{2,6}\mathbf{TE}_6] \\ \lambda_{3,1}\mathbf{T}_{\text{left}} + \lambda_{3,6}\mathbf{T}_{\text{right}} - [\lambda_{3,1}\mathbf{TE}_1 + \lambda_{3,2}\mathbf{TE}_2 + \lambda_{3,3}\mathbf{TE}_3 + \lambda_{3,4}\mathbf{TE}_4 + \lambda_{3,5}\mathbf{TE}_5 + \lambda_{3,6}\mathbf{TE}_6] \\ \lambda_{4,1}\mathbf{T}_{\text{left}} + \lambda_{4,6}\mathbf{T}_{\text{right}} - [\lambda_{4,1}\mathbf{TE}_1 + \lambda_{4,2}\mathbf{TE}_2 + \lambda_{4,3}\mathbf{TE}_3 + \lambda_{4,4}\mathbf{TE}_4 + \lambda_{4,5}\mathbf{TE}_5 + \lambda_{4,6}\mathbf{TE}_6] \\ \lambda_{5,1}\mathbf{T}_{\text{left}} + \lambda_{5,6}\mathbf{T}_{\text{right}} - [\lambda_{5,1}\mathbf{TE}_1 + \lambda_{5,2}\mathbf{TE}_2 + \lambda_{5,3}\mathbf{TE}_3 + \lambda_{5,4}\mathbf{TE}_4 + \lambda_{5,5}\mathbf{TE}_5 + \lambda_{5,6}\mathbf{TE}_6] \\ \lambda_{6,1}\mathbf{T}_{\text{left}} + \lambda_{6,6}\mathbf{T}_{\text{right}} - [\lambda_{6,1}\mathbf{TE}_1 + \lambda_{6,2}\mathbf{TE}_2 + \lambda_{6,3}\mathbf{TE}_3 + \lambda_{6,4}\mathbf{TE}_4 + \lambda_{6,5}\mathbf{TE}_5 + \lambda_{6,6}\mathbf{TE}_6] \end{pmatrix} \tag{A.13}$$

Eq. (A.13) is equated to zero based on the fact that when the truncation errors are included in the solution the numerical solution should match the analytical solution. Rearranging Eq. (A.13) and expressing it in vector and matrices form.

$$-\mathbf{A}^{-1}\mathbf{TE} = \mathbf{T} - \mathbf{T}_{\mathbf{FDM-CVF}} = \mathbf{Error} \tag{A.14}$$

Therefore, the value of the truncation errors can be obtained by.

$$\mathbf{TE} = \mathbf{A}(\mathbf{T}_{\mathbf{FDM-CVF}} - \mathbf{T}) = \mathbf{A}(-\mathbf{Error}) \tag{A.15}$$

Eq. (A.15) indicates that to calculate the truncation error vector for a one-dimensional, steady state, and linear differential equation with uniform mesh size, the negative of the error vector of the numerical solution (difference between the numerical solution and the analytical solution) should multiply the coefficient matrix (obtained for the discretised equation).

Truncation error for FDM:

The coefficient matrix **A** can be obtained by defining some jacobians:

$$\bar{B}_j = \frac{\partial F_j}{\partial \phi_j} \quad \bar{A}_j = \frac{\partial F_j}{\partial \phi_{j-1}} \quad \bar{D}_j = \frac{\partial F_j}{\partial \phi_{j+1}} \quad \bar{X}_j = \frac{\partial F_j}{\partial \phi_{j+2}} \quad \bar{Y}_j = \frac{\partial F_j}{\partial \phi_{j-2}} \tag{A.16}$$

therefore,

$$A = \begin{pmatrix} \bar{B}_1 & \bar{D}_1 & \bar{X}_1 & 0 & L & 0 \\ \bar{A}_2 & \bar{B}_2 & \bar{D}_2 & 0 & L & 0 \\ 0 & \bar{A}_j & \bar{B}_j & \bar{D}_j & \ldots & 0 \\ \vdots & \vdots & \vdots & \vdots & \vdots & \vdots \\ 0 & 0 & 0 & \bar{A}_{nj-1} & \bar{B}_{nj-1} & \bar{D}_{nj-1} \\ 0 & 0 & 0 & \bar{Y}_{nj} & \bar{A}_{nj} & \bar{B}_{nj} \end{pmatrix}_{nj \times nj} \tag{A.17}$$

Substituting Eq. (A.17) into Eq. (A.15) and evaluating.

$$\begin{aligned} TE_1 &= \bar{B}_1 E_1 + \bar{D}_1 E_2 + \bar{X}_1 E_3 \\ &\vdots \\ TE_j &= \bar{A}_j E_{j-1} + \bar{B}_j E_j + \bar{D}_j E_{j+1} \\ &\vdots \\ TE_{nj} &= \bar{Y}_{nj} E_{nj-2} + \bar{A}_{nj} E_{nj-1} + \bar{B}_{nj} E_{nj} \end{aligned} \tag{A.18}$$

Eq. (A.18) allows calculating the total truncation error at each node point for a one-dimensional, steady state, linear differential equation using FDM with uniform mesh size for any possible combination of the boundary conditions. The truncation error at a given node point is given by a linear combination of the error at that node and the errors at the nodes next to it (backward and forward to the node for central nodes, two nodes forward for the first node, and two nodes backward for the last node).

Truncation error for CVF:

For the CVF the jacobians calculated from $\bar{X}_1$ and $\bar{Y}_{nj-2}$ are equal to zero, therefore the total truncation errors at each node point are given by

$$\begin{aligned} TE_1 &= \bar{B}_1 E_1 + \bar{D}_1 E_2 \\ &\vdots \\ TE_j &= \bar{A}_j E_{j-1} + \bar{B}_j E_j + \bar{D}_j E_{j+1} \\ &\vdots \\ TE_{nj} &= \bar{A}_{nj} E_{nj-1} + \bar{B}_{nj} E_{nj} \end{aligned} \quad (A.19)$$

The truncation errors calculated from Eq. (A.19) represent the total truncation error at each node point. The equation can be used for any kind of boundary conditions using the CVF for a one-dimensional, steady state, linear differential equation with uniform mesh size discretisation.

References

Abell, M. L., & Braselton, J. P. (1994). *The maple V handbook*. New York: AP Professional.

Baek, S. W., Kim, M. Y., & Kim, J. S. (1998). Nonorthogonal finite volume solutions of radiative heat transfer in a three dimensional enclosure. *Numerical Heat Transfer B-Fundamentals*, *34*, 419.

Bird, R., Stewart, W., & Lightfoot, E. (1960). *Transport phenomena*. New York: Wiley.

Castillo, J. E., Hyman, J. M., Shashkow, M. J., & Steinberg, S. (1995). The sensitivity and accuracy of fourth order finite-difference schemes on nonuniform grids in one dimension. *Computers and Mathematics with Applications*, *30*, 41.

Chan, C. T., & Anastasiou, K. (1999). Solution of incompressible flows with or without a free surface using the finite volume method on unstructured triangular meshes. *International Journal of Numerical Methods Florida*, *29*, 35.

Ciarlet, P. G., & Lions, J. L. (1990). *Handbook of numerical analysis*, vol. 1. New York: Elsevier.

Cordero, E., De Biase, L., & Pennati, V. (1997). A new finite volume method for the solution of convection–diffusion equations: analysis of stability and convergence. *Communication Numerical Methods Engineering*, *13*, 923.

Davis, M. E. (1984). *Numerical methods and modeling for chemical engineers*. New York: Wiley.

Fan, D., & White, R. E. (1991). Optimization and extension of pentadioagonal BAND(J) solver to multiregion systems containing interior boundaries. *Computers and Chemical Engineering*, *15*, 797.

Johnson, R. W., & Mackinnon, R. J. (1992). Equivalent versions of the QUICK scheme for finite-difference and finite-volume numerical methods. *Communications in Applied Numerical Methods*, *8*, 841.

Leonard, B. P. (1994). Comparison of truncation error of finite difference and finite volume formulations of convection terms. *Applied Mathematical Modelling*, *18*, 46.

Leonard, B. P. (1995). Order of accuracy of QUICK and related convection–diffusion schemes. *Applied Mathematical Modelling*, *19*, 640.

Leonard, B. P., & Mokhtari, S. (1990). Beyond first-order upwinding: the ultra-sharp alternative for non-oscillatory steady-state simulation of convection. *International Journal for Numerical Methods in Engineering*, *30*, 729.

Marchuk, G. I. (1959). *Numerical methods for nuclear reactor calculations*. New York: Consultants Bureau.

Mathcad7, (1997). *User's guide*. Cambridge: MathSoft Inc.

Moder, J. P., Chai, J. C., Parthasarathy, G., Lee, H. S., Patankar, S. V. (1996). Nonaxisymmetric radiative transfer in cylindrical enclosures. *Numerical Heat Transfer B-Fundamentals*, *30*, 437.

Munz, C. D., Schneider, R., Sonnendrucker, E., Stein, E., Voss, U., & Westermann, T. (1999). A finite volume particle in cell method for the numerical treatment of Maxwell–Lorentz equations on boundary-fitted meshes. *International Journal for Numerical Methods in Engineering*, *44*, 461.

Newman, J. S. (1967). Numerical solution of coupled ordinary differential equations. University of California, Berkeley, UCRL-177369.

Newman, J. S. (1968). Numerical solution of coupled ordinary differential equations. *Industrial Engineering and Chemical Fundamentals*, *7*, 514.

Newman, J. S. (1973a). *Electrochemical systems*. New Jersey: Prentice-Hall.

Newman, J. S. (1973b). The fundamental principles of current distribution and mass transfer in electrochemical cells. *Electro-analytical Chemistry*, *6*, 187.

Noh, H. K., & Song, K. S. (1998). Temperature distribution of a low temperature heat pipe with multiple heaters for electronic cooling. *ETRI Journal*, *20*, 380.

Patankar, S. (1980). *Numerical heat transfer and fluid flow*. New York: Hemisphere Publishing.

Pozrikidis, C. (1997). *Introduction to theoretical and computational fluid dynamics*. New York: Oxford University Press.

Pozrikidis, C. (1998). *Numerical computation in science and engineering*. New York: Oxford University Press.

Shahcheragui, N., & Dwyer, H. A. (1998). Fluid flow and heat transfer over a three-dimensional spherical object in a pipe. *Journal of Heat Transfer-T. American Society of Mechanical Engineers*, *120*, 985.

Sohankar, A., Norberg, C., & Davison, L. (1999). Simulation of three dimensional flow around a square cylinder at moderate Reynolds numbers. *Physical fluids*, *11*, 288.

Stark, R. H. (1956). Rates of convergence in numerical solution of the diffusion equation. *Journal of Association of Computer Machines*, *3*, 29.

Su, M. D., Tang, G. F., & Fu, S. (1999). Numerical simulation of fluid flow and thermal performance of a dry cooling tower under cross wind condition. *Journal Wind Engneering and Industrial Aerodynamics*, *79*, 289.

Thynell, S. T. (1998). Discrete-ordinates method in radiative heat transfer. *International Journal of Engineering Sciences*, *36*, 1651.

Tikhonov, A. N., & Samarskii, A. A. (1956). On finite difference methods for equation with discontinuous coefficients. *Doklady Akad. Nauk SSSR* (*N.S.*), *108*, 393.

Van Zee, J., Kleine, G., & White, R. E. (1984). Extension of Newman's numerical technique to pentadiagonal systems of equations. In R. E. White, *Electrochemical cell design*. New York: Plenum Press.

Varga, R. S. (1957). Numerical solution of the two-group diffusion equation in x–y geometry. *IRE Transactions of the Professional Group on Nuclear Science*, NS-4, 52.

Varga, R. S. (1965). *Matrix iterative analysis*. New Jersey: Prentice-Hall.

Versteeg, H. K., & Malalasekera, W. (1995). *An introduction to computational fluid dynamics. The finite volume method*. Malaysia: Longman Group.

Vijayan, P., & Kallinderis, Y. (1994). A 3-D finite volume scheme for the euler equations on adaptive tetrahedral grids. *Journal of Computer Physics*, *113*, 249.

Wachspress, E. L. (1960). The numerical solution of boundary value problems. In A. Ralston, & H. S. Wilf, *Mathematical methods for digital computers*. New York: Wiley.

West, A., & Fuller, T. (1996). Influence of rib spacing in proton-exchange membrane electrode assemblies. *Journal of Applied Electrochemistry*, *26*, 557.

West, A., Yang, D., & Debecker, B. (1995). The simulation of mass-transfer effects for electrochemical-cell design. In *Electrochemical society proceedings*, vol. 95-11 (p. 172). Pennington: The Electrochemical Society.

White, R. E. (1987). Application and explanation of Newman's BAND(J) subroutine. Texas A&M University, Unpublished (available upon request).